HOCHSCHULE MITTWEIDA
UNIVERSITY OF APPLIED SCIENCES

Bachelor thesis

Emira Shehabi

Analysis of the neuron-specific expression of human amyloid precursor protein in the hippocampus of transgenic mice with amyloid pathology

Mittweida, 2017

Faculty of Applied Computer Sciences and Biosciences

Bachelor thesis

Analysis of the neuron-specific expression of human amyloid precursor protein in the hippocampus of transgenic mice with amyloid pathology

Author:
Emira Shehabi

Course of studies:
Biotechnology

Seminar group:
BT14wM-B

First examiner:
Prof. Dr. Röbbe Wünschiers

Second examiner:
Prof. Dr. Steffen Roßner

Submission: 28.08.2017

Bibliographic description:

Shehabi, Emira:

Analysis of the neuron-specific expression of human amyloid precursor protein in the hippocampus of transgenic mice with amyloid pathology.

Analyse der neuronenspezifischen Expression des humanen Amyloidvorläuferproteins im Hippokampus von Mäusen mit Amyloid-Pathologie.

Number of pages: 76.

University of Applied Sciences Mittweida

Bachelor thesis, 2017.

Contents

List of figures

List of tables

List of abbreviations

AD	Alzheimer's disease
APP	Amyloid precursor protein
A-β	Amyloid-β
BSA	Bovine serum albumin
CA	Cornu ammonis
CaBPs	Calcium-binding proteins
cAMP	Cyclic adenosine monophosphate
CB	Calbindin
CM	Calmodulin
CNS	Central nervous system
CR	Calretinin
DG	Dentate gyrus
DIFS	Double immunofluorescence stain
GABA	γ-aminobutyric acid
hAPP	Human APP
HRP	Horseradish peroxidase
IHC	Immunohistochemistry
iAβ	Intraneuronal A-β
sAPP	Soluble APP
PBS	Phosphate-buffered saline
PSEN1	Presenilin 1
PV	Parvalbumin
SST	Somatostatin
TBS	Tris-buffered saline

1 Introduction

1.1 Overview

Covering approximately $^2/_3$ of all dementia cases, Alzheimer's disease (AD) represents the most common form of dementia. Usually affecting people of the age range of 65 and above, it is significantly higher spread in individuals of the female gender.[1] There are approx. 1.2 million people in Germany alone, suffering from the fatal symptoms of this neurodegenerative disease.[2,3] The symptoms start with short-term memory loss, later leading to a complete impairment of cognition and language due to damaged neurons and tissue degeneration in parts of the brain realizing cognitive functions such as the cortex and hippocampus. Caused by these severe changes in the brain, patients often show behavioural impairments, mood swings and changes in personality.[4]

The neuropathology of AD was thought to be primarily characterized by the extracellular generation and deposition of amyloid-β (A-β) peptides in the brain, first forming oligomers which then accumulate to A-β plaques. However, more recent evidence indicates that A-β can accumulate intracellularly in neurons, too.[5] Toxic versions of A-β peptides are generated through abnormal processing of human amyloid precursor protein (hAPP). Initiating in the entorhinal cortex and hippocampus, the pathology then spreads across other parts of the central nervous system (CNS) causing the death of neurons and leading to shrinkage of the brain. To this day, the pharmaceutical market can only offer drugs which reduce some of the symptoms of AD. An effective cure, targeting the underlying molecular mechanisms of AD has yet to be found. For this reason, researchers study the effects of AD in the brain with the help of model organisms, especially

[1] Juan Yang et al.: "Induced pluripotent stem cells in Alzheimer's disease: applications for disease modeling and cell-replacement therapy"

[2] Alzheimer Forschung Initiative e.V.: "Zahlen und Fakten der Alzheimer-Krankheit in Deutschland"

[3] Statista - Universität Leipzig: "Statistiken zur weltweiten Verbreitung von Demenz"

[4] Juan Yang et al.: "Induced pluripotent stem cells in Alzheimer's disease: applications for disease modeling and cell-replacement therapy"

[5] Minho Moon et al.: "Intracellular amyloid-β accumulation in calcium-binding protein-deficient neurons leads to amyloid-β plaque formation in animal model of Alzheimer's disease"

transgenic rodents.[6] The transgenic mice and rats are genetically modified to overexpress abnormal versions of hAPP to develop common neuropathology traits of AD.[7] Not genetically modified mice and rats naturally contain endogenous murine APP, but show an absence of toxic amyloid-β deposits which affects the formation of secondary structures, such as oligomers. Caused by the differences in neuropathologic traits, the typical symptoms and impacts on brain functions, such as memory and behaviour, can't be observed in mouse models.[8]

Although there are differences in the amino acid sequence between hAPP and murine APP, antibodies available on the market can't differentiate between these two proteins, making it impossible to study and prove the expression patterns of hAPP in mice.[9] Corinna Höfling and colleagues have therefore developed and characterized two monoclonal antibodies 1D1 and 7H6 that recognize only human APP by immunological methods, such as immunohistochemistry and Western Blot, but also in in vivo applications. With the help of the newly developed antibodies, hAPP-expressing interneurons in the hippocampus can be studied, which have been found to play a rather important role in AD.[10,11]

1.2 The human brain

Protected from the skull lies the brain, the part of the body responsible for emotions, memories and thoughts. Weighing about 1.0 to 1.5 kg, it contains about 100 billion nerve cells and consists of three main sections: the cerebrum, cerebellum, and brain stem.[12]

[6] Corinna Höfling et al.: "Differential transgene expression patterns in Alzheimer mouse models revealed by novel human amyloid precursor protein-specific antibodies"

[7] U.S. National Library Of Medicine: "PSEN1 gene"

[8] Corinna Höfling et al.: "Differential transgene expression patterns in Alzheimer mouse models revealed by novel human amyloid precursor protein-specific antibodies"

[9] Ibid.

[10] Ibid.

[11] Rice University: "Hippocampus"

[12] Mayfield Clinic: "Anatomy of the Human Brain"

As illustrated in figure 1, the cerebrum is the largest part of the brain, containing about 70% of all nerve cells. It can be divided into the right and left hemisphere, each controlling different functions that are crucial in our everyday lives. The dominant, left hemisphere primarily controls language and speech while the right hemisphere is assigned to spatial processing and interprets visual information transmitted from our eyes. Those hemispheres are joined by a bundle of fibres called *corpus callosum*, allowing them to exchange information. The left and right hemisphere again are divided into four lobes: the frontal, parietal, occipital and temporal lobe. Connected with each other, they function jointly.[13]

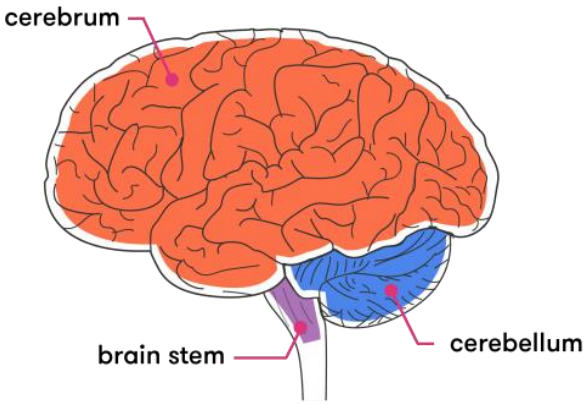

Figure 1: *The main sections of the brain: the cerebrum, cerebellum and brain stem. Source: http://www.nova.org.au/sites/default/files/images/people-and-medicine/brain/brain-illustrations-02-v6_670x449.png. Status: 28.04.2017.*

The folded tissue top of the cerebrum called the cortex or neocortex allows more neurons to exist due to the increased surface. It contains about 70% of all nerve cells in our brain. Underneath the cerebrum lies the cerebellum, functioning as a coordinator of muscle movements, posture and balance. Connecting the cerebellum and cerebrum to the spinal cord, the brain stem performs automatic functions such as breathing and controlling the heart rate and body temperature. It can be divided into the midbrain, pons and medulla.

[13] Ibid.

The cerebellum, pons and medulla form a structure called the hindbrain. Located deep in the brain lie other essential structures that are mostly responsible for automatic functions, such as the limbic system. It is composed of the hypothalamus, thalamus, amygdala, hippocampus, and pituitary gland, as seen in figure 2.[14]

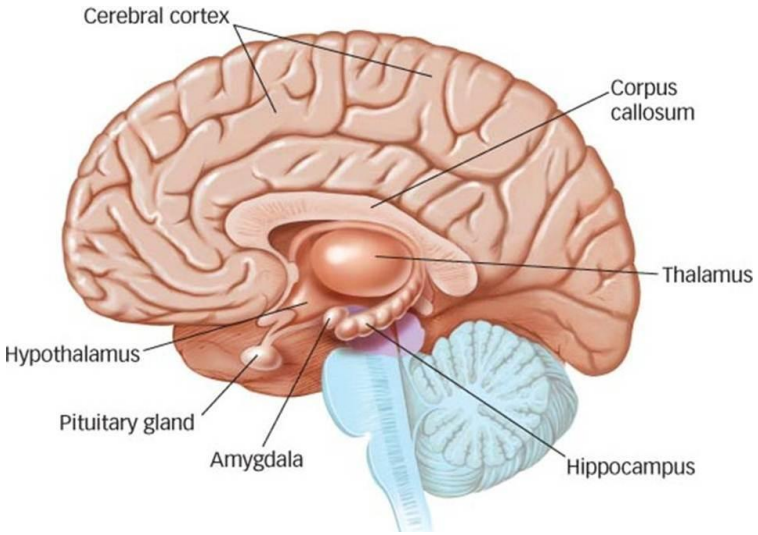

Figure 2: *The components of the limbic system, shown with the cerebral cortex and corpus callosum. The corpus callosum is the largest bundle of nerve fibres, containing over 200 million axons. Its function is to connect the brain's cerebral hemispheres.[15]. Source: http://classconnection.s3.amazonaws.com/252/flashcards/1048252/png/forebrain1328987872235.png. Status: 28.04.17.*

Learning and memory formation are very important processes in the central nervous system. They lead to a 'rewiring' of the network, through structural reconfiguration of synapses induced by activity-change of certain neurons. This rewiring in form of establishment and elimination of synapses is a process necessary for the brain to adapt to new environments. [16] Different areas of our brain are involved in storing information in form of memories. When a person achieves a new skill, it is stored as an automatic

[14] Ibid.

[15] David Hubel: "Eye, Brain, and Vision"

[16] Lena C. Schmid et al.: "Dysfunction of Somatostatin-Positive Interneurons Associated with Memory Deficits in an Alzheimer's Disease Model"

memory in the cerebellum. Short-term memories are saved in the prefrontal cortex for about a minute. Long-term memories on the other hand can be kept for a longer time, since it has an almost unlimited content and duration capacity in the hippocampus.[17] Additionally, the hippocampus controls spatial navigation and is therefore the part of the brain where AD -symptoms, which include memory problems and disorientation, start to appear. Due to the organized anatomic structure in the hippocampus, it is used as a model system for neurophysiology studies.[18]

1.3 The rodent brain

The brain of a rodent differs most prominently in its structure, which doesn't appear as complex as the human one. When comparing both brain structures, one can also notice a prominent area in the rodent brain, which is less distinguished in humans: the olfactory bulb. Rodents, as many other mammalians, rely on their olfactory sensibility for viability. With the help of this organ, they can distinguish toxic from 'neutral' food, but it also influences sensing of predators and possible mating partners. Even though the olfactory bulb represents one of the most essential and basic parts of the brain, it appears to be very complex. To describe the ends of the rodent brain, the anatomical terms 'rostral' and 'caudal' are used; the olfactory bulb is therefore on the rostral side and the hindbrain on the caudal (illustrated in figure 3). [19] Sectioned tissue slices from the caudal and rostral side of the rodent brain differ most obviously in the hippocampus area, which is much larger on the caudal side (as seen in figure 3).

[17] Mayfield Clinic: "Anatomy of the Human Brain"

[18] Rice University: "Hippocampus"

[19] Christof Koch and R. Clay Reid: "Neuroscience: Observatories of the mind"

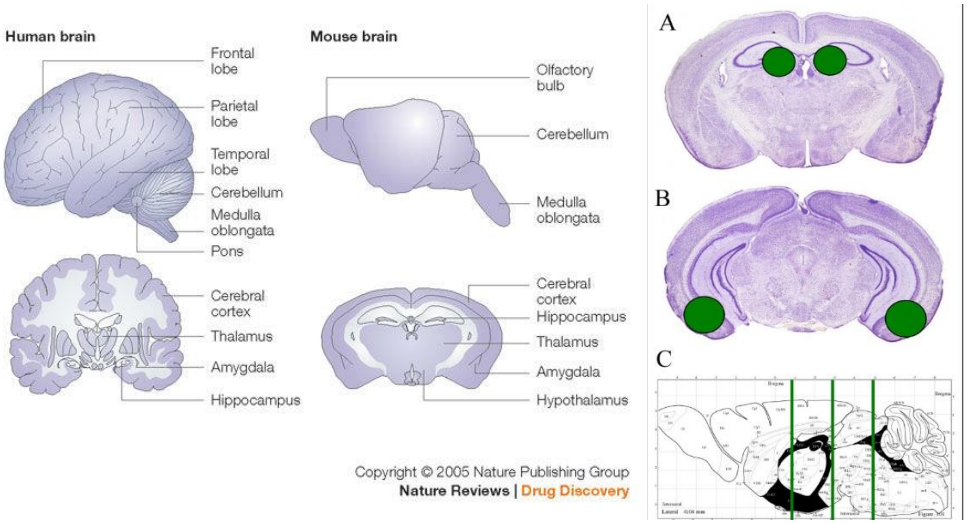

Figure 3: *Comparison of the human and mouse brain in a lateral and sectioned view (left). Right picture depicts the whole lateral brain and sectioned brain tissue. The rostral area is on the side of the olfactory bulb, whereas the hindbrain side represents the caudal area.*[20] *A) Rostral brain area. B) Caudal brain area.*[21] *Source: http://www.getdomainvids.com/rdg.html? Status: 15.08.2017.*

Because the rodent brain anatomy is so different, especially in the parts associated with higher cognitive function, neurological disorders such as Alzheimer's disease do not trail the exact same pathological paths as in the human brain. For this reason, animal models will probably ever be able to mimic the aspects and traits of a human neurological disease to only a certain extent, solely by the fact that their mentality is not comparable to ours.

1.4 Interneurons

As seen in figure 4, the hippocampus of rodents and humans is a bilaminar structure consisting of the dentate gyrus (DG) and cornu ammonis (CA) which is also called the hippocampus proper.

[20] Joanne Mayer, Michelle G. Hamel and Paul E. Gottschall: "Evidence for proteolytic cleavage of brevican by the ADAMTSs in the dentate gyrus after excitotoxic lesion of the mouse entorhinal cortex"

[21] Ibid.

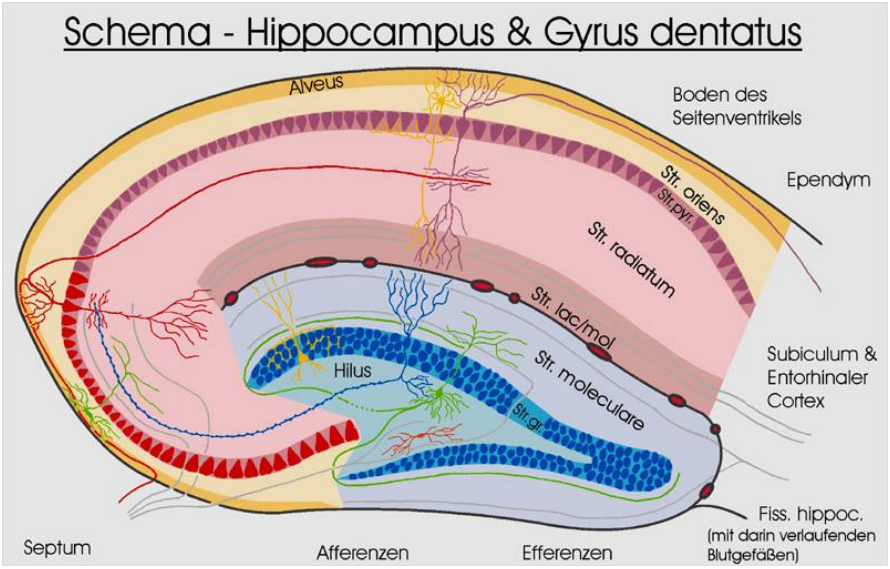

Figure 4: *The layers of the hippocampus in mice: Alveus, stratum oriens, stratum pyramidale, stratum radiatum, stratum lacunosum moleculare and the dentate gyrus. Original picture: http://anatomie.vetmed.uni-leipzig.de/external/hippocampus/index.html. Status: 28.04.17.*

Both structures are separated into multiple layers that can be differentiated under the microscope. The CA consists of four fields CA1 to CA4, which are necessary to describe the cell layers in different positions of the cornu ammonis. One of the most prominent layers is the stratum pyramidale. The pyramidal cells in this layer represent the cornu ammonis' principal cells, which are major sources of output to the rest of the brain like all other principal cells. The name of these cells derives from the triangular soma, which allows for a quick and certain identification. [22]

Together with the stratum lacunosum and the stratum moleculare in the dentate gyrus, these layers contain the highest number of so called interneurons in the hippocampus.[23] Interneurons, owning diverse morphological, physiological, molecular and synaptic characteristics, make up about 25% of cortical neurons. [24] Their neuron type is neither

[22] Henri M. Duvernoy, Françoise Cattin and Pierre-Yves Risold: *"The Human Hippocampus"*

[23] Ibid.

[24] Learn.Genetics: "The Other Brain Cells"

sensory, motoric nor projecting, but specialized with their primary role being the formation of connections between other types of neurons with the help of witch they transfer impulses throughout the CNS. These cells are mostly inhibitory, using γ-aminobutyric acid (GABA) as a neurotransmitter and are vital in the wiring and circuitry of developing nervous systems.[25] Released by electrically-stimulated inhibitory neurons, GABA turns the membrane potential more negative, hindering the neuron in reaching a threshold large enough to fire an action potential.[26,27] GABA and glutamate (a neurotransmitter of excitatory neurons) represent 90% of all neurotransmitters in the brain, hence a balance between the two is essential for a properly functioning CNS. Both neurotransmitters originate from glutamine, which, in glutamatergic neurons, is converted into glutamate through catalysis by phosphate-activated glutamine synthetase and glutaminase. In GABAergic, inhibitory neurons glutamate is further altered by decarboxylation catalysed with glutamate decarboxylase into GABA, as depicted in figure 5.[28] As GABA's main function, it opens ion channels that are permeable for chloride, bicarbonate or potassium ions in postsynaptic (occurring distal to a synapse) neurons, through inhibitory postsynaptic potential.[29,30] Chloride-channelling has the benefit of stabilizing the membrane potential to reach a negative near resting level, allowing the ion channels to recover.[31]

[25] Corey Kelsom and Wange Lu: "Development and specification of GABAergic cortical interneurons"

[26] Knowing Neurons: "Inhibitory Neurons: Keeping the Brain's Traffic in Check"

[27] RICHARD W. OLSEN: "GABA"

[28] Joanna M et al.: "The Loss of Glutamate-GABA Harmony in Anxiety Disorders"

[29] Learn.Genetics: "The Other Brain Cells"

[30] RICHARD W. OLSEN: "GABA"

[31] PhysiologyWeb Team: "Physiological Significance of the Membrane Potential"

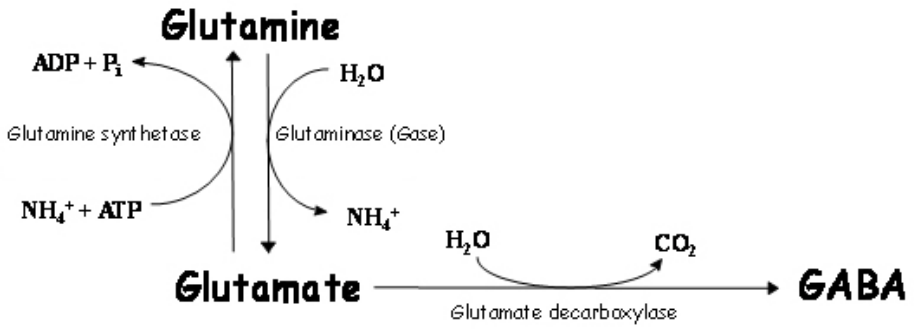

Figure 5: *In GABAergic and glutamatergic neurons glutamine is converted into glutamate through catalysis by phosphate-activated glutamine synthetase and glutaminase, whereas in GABAergic neurons glutamate is further converted into GABA by decarboxylation catalysed with glutamate decarboxylase.*[32] *Original picture: https://oatext.com/img/Glutamate-transporters-1.jpg; edited by Emira Shehabi. Status: 28.04.2017.*

The structure of a typical interneuron is illustrated in figure 6 and can be compared to the structure of a sensory neuron, showing the cell body with the nucleus at the centre and the dendrites, axon and synaptic endings with which the interneuron connects to other neurons in the brain. Sensory, motor and interneurons have similar structures, but differ in function. While interneurons connect neurons, sensory neurons gather information from sensory organs and motor neurons carry impulses from the brain and the spinal cord to muscles.[33]

[32] Joanna M et al.: "The Loss of Glutamate-GABA Harmony in Anxiety Disorders"

[33] Scientific American Blog Network: "Know Your Neurons: How to Classify Different Types of Neurons in the Brain's Forest"

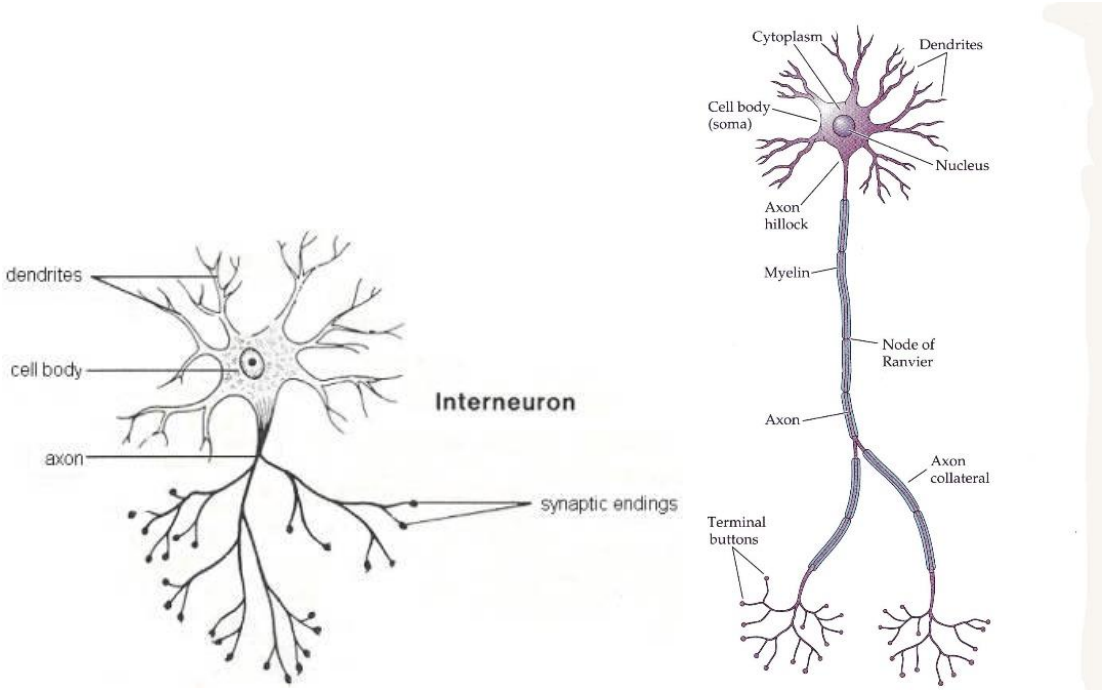

Figure 6: *The structure of an interneuron (left) and of a sensory neuron (right). Source:* http://www.biologymad.com/nervoussystem/relayneurone.jpg *(left);* http://classtalkers.com/wp-content/uploads/2011/11/structure_of_a_neurone1.jpg (right). *Status: 24.08.2017.*

The functions of interneurons are still not completely understood, but studies show that they could play a vital role in modulating cortical output and plasticity and that they are possibly specialized to target different parts of neurons, because of their excitatory and inhibitory characteristics. Regarding AD, researchers have found the characterization of interneuron types and their location to be very important for research that focuses on developing new drug therapies against the disease. The study described interneurons as rather vulnerable to AD -related damage, since certain interneurons express abnormally high levels of APP which leads to the formation of neurotoxic A-β oligomers and amyloid plaques. A small number of damaged interneurons can already cause memory and learning impairments, accelerating the course of the disease. [34]

Interneurons typically express many neuropeptides and calcium-binding proteins (CaBPs) such as calmodulin (CM), calretinin (CR), calbindin (CB) and parvalbumin

[34] Heather Caroline Rice: "Selective Vulnerability of Interneurons in Alzheimer's Disease"

(PV). These proteins can be used to mark pathways and cells with the help of specific antibodies that detect them. CM is the most distributed CaBP. It affects several Ca^{2+}-dependent regulations of enzymes and cell processes by binding Ca^{2+} to all four of its binding sites. CB protects neurons from being flooded with calcium-ions, which can occur, when damaged neurons spill out glutamate into neighbouring areas and cause cell death. [35] It has been reported to occur in 10-20% of GABAergic interneurons in the hippocampus.[36] One of the least abundant CaBPs is CR, due to only 13% of GABAergic interneurons in the mouse being CR -positive.[37] Functioning as a regulator of other GABAergic inhibitory interneurons, it additionally regulates the excitatory action of principal cells. Neuroscientific research has discovered a selective vulnerability of CR-positive interneurons to neurodegeneration induced by A-β deposits. But only severe AD -cases have shown a significantly reduced density of CR -positive interneurons in the hippocampus. [38] PV has a similar function and structure to CM. Because of its usual colocalization with GABA, it is used as a marker for subpopulations of GABAergic neurons. [39] Around 32-38% of GABAergic interneurons in the hippocampus of the mouse are PV -positive.[40] Named basket cells due to their widely reaching dendrites, these cells can fire action potentials at a high rate while concurrently having short recovery times.[41] Experiments in an AD -model have shown that restoration of PV -positive inhibitory neurons led to better performance in memory tasks. PV -positive interneurons can therefore be regarded as actively involved in learning and memory formation.[42] These CaBPs occur in certain subpopulations of neurons in the brain, such as in the interneurons

[35] Andressen C. et al: “Calcium-binding proteins: selective markers of nerve cells.”

[36] Dhiraj Maskey et al.: “Changes in the distribution of calbindin D28-k, parvalbumin, and calretinin in the hippocampus of the circling mouse”

[37] Ibid.

[38] David Baglietto-Vargas et al.: “Calretinin interneurons are early targets of extracellular amyloid-beta pathology in PS1/AbetaPP Alzheimer mice hippocampus”

[39] Andressen C. et al.: “Calcium-binding proteins: selective markers of nerve cells.”

[40] Dhiraj Maskey et al.: “Changes in the distribution of calbindin D28-k, parvalbumin, and calretinin in the hippocampus of the circling mouse”

[41] Knowing Neurons: “Inhibitory Neurons: Keeping the Brain’s Traffic in Check”

[42] Lena C. Schmid et al.: “Dysfunction of Somatostatin-Positive Interneurons Associated with Memory Deficits in an Alzheimer’s Disease Model”

of the hippocampal area. Utilizing antibodies against CaBPs in immunohistochemical methods, targeted areas in the brain can be marked where these proteins reside.[43]

An interneuronally expressed neuropeptide is e.g. somatostatin (SST). It is also produced in other neurons and secretory cells in the central and peripheral nervous system and gastrointestinal tract and released by membrane depolarization or increasing Ca^{2+} -concentration in the cell. Its function is to inhibit secretion of neurotransmitters or hormones. Many hormones, neuropeptides, neurotransmitters, nutrients and other compounds stimulate SST -secretion, while opiates and GABA usually play an inhibiting role.[44] Studies have shown the importance of SST in AD, stating that a single nucleotide polymorphism in the SST -gene can already increase AD -risk. [45]

1.4.1 Morphology of interneurons

Inhibitory interneurons show big differences in somatic, dendritic and axonal morphologies, but vary the most in their dendritic morphology, by which they cannot be reliably defined. Only the axonal morphology can securely identify the interneuron type, due to the fact that interneurons seem to target different domains of neurons. Interneurons can be subdivided into basket, double bouquet, bipolar, bitufted, martinotti and chandelier cells, as shown in figure 7.

[43] Andressen C. et al: “Calcium-binding proteins: selective markers of nerve cells.”

[44] Noemí Bronstein-Sitton: “Somatostatin and the Somatostatin Receptors”

[45] Yadong Huang and Lennart Mucke: “Alzheimer mechanisms and therapeutic strategies”

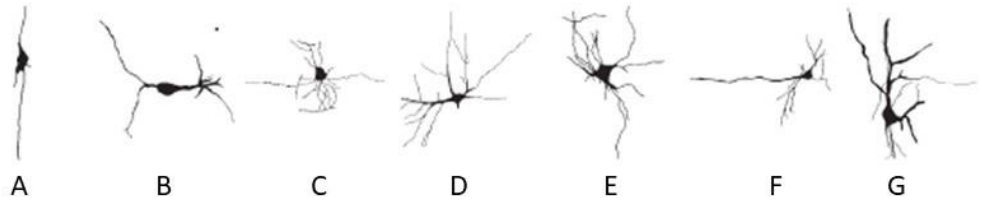

Figure 7: *Different morphologic appearances of interneurons. (A) Horizontal neuron. (B) Bitufted neuron. (C) Chandelier neuron. (D) Basket neuron. (E) Aspiny stellate cell. (F) Pyramidal neuron. (G) Martinotti cell. Source:[46]; edited by: Emira Shehabi. Status: 31.07.2017.*

Approximately 50% of inhibitory neurons are of the basket cell type. They target the somata and proximal dendrites of pyramidal neurons and interneurons. Because of innervation by many basket cells, they exhibit a basket-like appearance around pyramidal cell somata. They can be subdivided into large, small and nest basket cells, expressing many neuropeptides and the CaBPs PV and CB. Large basket cells have larger dendrites than the other two basket cell types and expansive axonal arborizations. They typically express CB, PV and occasionally SST and CR. Chandelier cells target axons and are named after their chandelier-like appearance, which seems to take clearer forms in higher specimens, such as primates. They express parvalbumin, calbindin or even both CaBPs. Martinotti cells target proximate and distal dendrites and somata. They appear bitufted with a more elaborate dendritic tree than other interneurons and typically express the neuropeptide SST. Bipolar cells are small with spindle or ovoid somata and express CR, while double bouquet cells appear with a bitufted dendritic morphology and express CB, CR or both together. Bitufted cells, on the other hand, are characterized by their ovoid somata and wide horizontal axonal spans. Targeting dendrites, they express CB, CR and SST. [47]

[46] C. Pesold et al.: “Cortical bitufted, horizontal, and Martinotti cells preferentially express and secrete reelin into perineuronal nets, nonsynaptically modulating gene expression”

[47] Henry Markram et al.: “Interneurons of the neocortical inhibitory system”

1.4.2 Colocalization

Neuropeptides and CaBPs can colocalize with other compounds or with each other in neurons and interneurons. The term colocalization, as a biological designation, describes two or more different compounds that are located in the same spot in an organism. When used in the context of tissue, colocalization of two molecules could mean joint sharing of the same receptor. In the context of fluorescent microscopy, it refers to fluorescent molecules, whose colours share the same pixel in the image. By means of double immunofluorescent staining, two or more different, fluorescently-labelled molecules can be marked and the possibility of colocalization investigated with a fluorescent microscope through overlay of fluorescent filters. Examining possible physical co-occurrence of compounds is very important for the analysis of biological interactions. [48]

Interneurons have the ability to co-express up to five different neuropeptides and CaBPs. Many of those molecules appear to be expressed independently of each other like CB, which can be seen colocalizing with many neuropeptides and other CaBPs. Regarding CaBPs, calbindin, calretinin and parvalbumin are primarily expressed separately in different populations of interneurons. In some cases, expressions of some of those CaBPs overlap and result in colocalizing compounds. Calbindin and parvalbumin occasionally are found to co-occur, while the combination of calbindin and calretinin is rarer.[49]

The three CaBPs occur mostly in three broad interneuron classes: PV in fast-spiking, CB in bursting and CR in accommodating or irregular-spiking interneurons. But because more than three anatomical, electrical and combined types exist, these proteins can't be assigned to only one interneuron class and therefore colocalization occurs.[50]

1.5 Pathology of Alzheimer's disease and its animal models

Amyloid-β peptides occur naturally through cleavage of APP by β- and γ-secretase. BACE1 or β-secretase is essential for the cleavage of APP, because it initiates A-β -

[48] Bywalez and Wolfgang: "Physiology of rodent olfactory bulb interneurons"

[49] Henry Markram et al.: "Interneurons of the neocortical inhibitory system"

[50] Ibid.

formation by producing the N-terminus of A-β. [51] Cleaving APP at its β-site, the enzyme generates the C-terminal fragment C99, which is membrane bound and subsequently processed by γ-secretase to release A-β. Due to the enzyme's necessity in the initiation of A-β -cleavage, it is a prime drug target for AD. [52] The γ-secretase cleaves transmembrane proteins in the brain thereby forming peptides, such as soluble APP (sAPP), a compound that can be neuroprotective and stimulate neurogenesis. The proteolytic function of this complex is assigned to the protein-subunit presenilin 1, which is encoded by the PSEN1 gene. According to studies, 70% of early-onset AD cases have mutations in their PSEN1 gene. More than 150 mutations of the PSEN1 gene, most of them point mutations, have been identified in these patients. The mutated gene produces abnormal presenilin 1 proteins, altering the function of γ-secretase, changing the processing of APP and causing an overproduction of longer, toxic versions of A-β peptides that form plaques in the hippocampus.[53] Formerly, extracellular formation of A-β has been assumed to be crucial for the formation of plaques in the brain. Recent research has shown evidence that A-β can also accumulate inside of neurons, which is even supposed to accelerate AD -progression. Here, intraneuronal A-β (iA-β) is accumulated and leads to the degeneration of the neuron, which secretes iA-β into the extracellular space, where it forms plaques. This evidence has been gathered in AD -patients and some transgenic animals, but it has not been investigated in transgenic AD -mouse models yet.[54]

Neurons exposed to high levels of toxic A-β peptides usually shrink, developing shorter dendrites with less dense spines. Increased turnover of dendrite spines has been observed in inhibitory neurons, lessening the amount of input that the neuron can achieve. The shrinkage can increase cellular excitability and thus production of glutamate, creating an imbalance between excitation and inhibition which could be the basis for neuronal

[51] Patty C. Kandalepas and Robert Vassar: "The Normal and Pathologic Roles of the Alzheimer's β-secretase, BACE1"

[52] Robert Vassar et al.: "The beta-secretase enzyme BACE in health and Alzheimer's disease: regulation, cell biology, function, and therapeutic potential"

[53] U.S. National Library Of Medicine: "PSEN1 gene"

[54] Minho Moon et al.: "Intracellular amyloid-β accumulation in calcium-binding protein-deficient neurons leads to amyloid-β plaque formation in animal model of Alzheimer's disease"

network dysfunction.[55,56] Additionally, toxic A-β peptides have been shown to decrease the number of synapses in the brain and inhibit proper structural remodelling of excitatory synapses and dendrites, which can explain AD -typical impairments in memory.[57]

To find therapeutic strategies that can reduce toxic A–β generation, transgenic mice have been developed that are used as AD -model organisms. These mice overexpress abnormal human APP (hAPP) and presenilin 1 proteins and thus develop many AD –features, such as A–β deposition and plaques, signs of neurodegeneration and memory impairment. One of the most used transgenic mouse models is the Tg2576 mouse. This transgenic mouse species overexpresses the hAPP -isoform with 695 amino acids and develops A–β plaques in the age of 9–10 months.[58] Due to simultaneous murine APP -production, the models show a difference in spatial and temporal appearance of toxic A–β deposits and synaptic dysfunction as well as discrepancies in impairments in memory and behaviour, resulting from the differences between murine and human APP.[59] Unfortunately, a full replication of the human disease is not possible due to absence of neurofibrillary tangles and little to no neuronal loss in the brains of experimental animals.[60]

1.6 Goal

The goal of this thesis was the detection and characterization of different types of hAPP -expressing interneurons in the hippocampus of transgenic mice. To achieve this goal the hAPP -specific antibody 1D1 was used in immunohistochemical methods. Emphasis was

[55] Jorge J. Palop and Lennart Mucke: “Network abnormalities and interneuron dysfunction in Alzheimer disease”

[56] Lena C. Schmid et al.: “Dysfunction of Somatostatin-Positive Interneurons Associated with Memory Deficits in an Alzheimer’s Disease Model”

[57] Ibid.

[58] Anniina Snellman et al.: “Longitudinal amyloid imaging in mouse brain with 11C-PIB: comparison of APP23, Tg2576, and APPswe-PS1dE9 mouse models of Alzheimer disease”

[59] Corinna Höfling et al.: “Differential transgene expression patterns in Alzheimer mouse models revealed by novel human amyloid precursor protein-specific antibodies”

[60] Anniina Snellman et al.: “Longitudinal amyloid imaging in mouse brain with 11C-PIB: comparison of APP23, Tg2576, and APPswe-PS1dE9 mouse models of Alzheimer disease”

given on the determination of the number of interneurons in hippocampal layers and their exact localization. Additionally, the calcium-binding proteins parvalbumin, calretinin and calbindin and the neuropeptide somatostatin were detected using the same methods to examine a possible colocalization of these proteins with hAPP in interneurons.

2 Material and equipment

2.1 Material

2.1.1 Buffers

Buffer	Ingredients/ Producer
Phosphate-buffered saline (PBS, 0,1 M, pH 7,4)	Na_2HPO_4: Roth NaH_2PO_4: Roth
PBS/ 0,025% Sodium azide (NaN_3)	Sodium azide (NaN_3): Sigma-Aldrich
Tris-buffered saline (TBS, 0,1 M, pH 7,4)	NaCl: Roth Tris: Roth
Tris Buffer (0,05 M, pH 7,6)	Tris: Roth

2.1.2 Other chemicals

Chemicals	Producer
Hydrogen peroxide (H_2O_2, 30%)	Merck Millipore
Triton X-100	FERAK
Methanol	J.T. Baker

Entellan®	Sigma-Aldrich
Toluene	Roth
Protein glycerol	Roth

2.1.3 Sera

Serum	**Producer**
Goat-normal serum	Dianova
Donkey-normal serum	Dianova
Bovine serum albumin (BSA)	SERVA

2.1.4 Primary antibodies

Antibody	**Producer**
Rat anti-human APP (clone 1D1 from supernatant of rat hybridoma cells)	Dr. Kuhn, TU Munich
Rabbit anti-parvalbumin	Swant

Rabbit anti-calbindin	Swant
Rabbit anti-calretinin	Swant
Goat anti-somatostatin	Swant

2.1.5 Secondary antibodies

Antibody	**Producer**
Donkey anti-rabbit (Cy2-conjugated)	Dianova
Donkey anti-goat (Cy2-conjugated)	Dianova
Donkey anti-rat (Cy3-conjugated)	Dianova

2.2 Preparation of buffers

Buffer	**Ingredients and preparation**
PBS (0,1 M, pH 7,4)	**<u>Solution A (0,2 M)</u>** $Na_2HPO_4 * 2\ H_2O$ 35,61 g Filled up with distilled water to 1 litre.

	Solution B: 0,2 M	
	$NaH_2PO4 * H_2O$	27,6 g
	Filled up with distilled water to 1 litre.	
	Preparation for solution of pH 7,4 (25°C):	
	Solution A Solution B	40,5 g 9,5 g
	Mixed and diluted to 100 ml with distilled water.	
TBS (0,1 M, pH 7,4)	Tris	12,1 g
	NaCl	8,8 g
	Filled up with distilled water to 1 litre.	

2.3 Equipment

Equipment and specific identifier	**Producer**
Vortex shakers:	
Vortex-Genie 2	Scientific Industries
Scales:	
Mettler AM50	Mettler
Mettler Toledo	Mettler

Centrifuges:	
1-14	Sigma
Optical microscopes:	
Stemi DV4	Zeiss
Axioplan 2	Zeiss
Fluorescence microscopes:	
BIOREVO BZ-9000	Keyence
Heat plates:	
RCTbasic	KIKA Labortechnik
Platform shaker:	
Duomax 1030	Heidolph
Thermoshaker:	
HC24N	Grant-bio

3 Methods

In order to examine the hippocampal interneurons of hAPP -transgenic mice, animals were sacrificed by CO_2 inhalation and perfused with PBS followed by 4% paraformaldehyde. The brains were prepared and the cerebrum was separated from the cerebellum and cut into 30 µm thin slices at about -40°C. The cut slices were immersed in wells filled with PBS and 0,025% $NaNO_3$.

In all following methods, the collected brain slices were washed in a microtiter plate filled with 0,1 M Tris-buffered saline (TBS, pH 7,4) 3 times for 5 minutes each time after every incubation step (unless stated otherwise). The plate was then placed on a platform shaker.

For every method, a certain number of brain tissue sections was used. The tissue was taken from hAPP -transgenic Tg2576 mice. Preferred were freshly cut brain sections from 3-month-old mice, because older mice display more background signal with a compound called lipofuscin, which is an 'aging pigment' that occurs after damaged blood cells have been broken down and absorbed.[61] The autofluorescence of these pigments in samples of aged animals complicates the analysis of stained interneurons. Furthermore, tissue from the caudal brain area was decided to be used, because of its large hippocampal area that exhibits a higher number of interneurons.

Table 1 contains every primary and secondary antibody that has been utilized in the methods except for rat anti-human APP (1D1) in the double immunofluorescence stains (DIFS), which was used in every stain in a dilution of 1:2. Targeting rat anti-human APP, the secondary antibody, Cy3 -conjugated donkey anti-rat was used.

The dilutions stated in table 1 have been suggested by the provider. Some dilutions have been changed during the experiments in this project, because of too weak/ intense background and interneuron staining results.

[61] MedlinePlus Medical Encyclopedia: "Lipofuscin"

Table 1: The utilized primary and secondary antibodies.

Method	Primary Antibody	Dilution	Secondary Antibody
DIFS hAPP/ Parvalbumin	Rabbit anti-parvalbumin	1:4000	Donkey anti-rabbit (Cy2-conjugated)
DIFS hAPP / Calretinin	Rabbit anti-calretinin	1:1000	Donkey anti-rabbit (Cy2-conjugated)
DIFS hAPP / Calbindin	Rabbit anti-calbindin	1:1000	Donkey anti-rabbit (Cy2-conjugated)
DIFS hAPP / Somatostatin	Goat anti-Somatostatin	1:200	Donkey anti-goat (Cy2-conjugated)

3.1 Double immunofluorescence staining

DIFS combines the two benefits of saving time, due to concurrent targeting of two antigens on one tissue, and the possibility of finding colocalising compounds, which could elucidate possible collaboration of these compounds in molecular mechanisms that may be crucial for the development or prevention of AD. DIFS utilizes a primary and a secondary antibody-cocktail. The secondary antibody-cocktail used in the following stains included antibodies conjugated to the cyanine fluorophores Cyanine (Cy2) and Indocarbocyanine (Cy3), which have excitation and emission peaks at different wavelengths that are listed in table 2. A signal-enhancing antibody-cocktail can be added after incubation with the secondary antibodies. Signal-enhancers in form of another Cy3-/Cy2 -conjugated secondary antibody and Streptavidin-Cy3 were tested on the tissue and resulted in a very intense background signal, which led to abolishment of the signal-enhancing step in the protocol. Additional testing of the cyanides was done, to determine the best fluorescent marker for hAPP. The tissue marked with Cy3 had a much more

intense fluorescent hAPP -stain, thus this cyanide was chosen to be utilized in every following double immunofluorescence method for marking hAPP. Consequently, the antibodies against CaBPs were conjugated with Cy2.

Every primary antibody-cocktail was diluted in TBS, 5% donkey-normal serum and 0,2% Triton X-100 and every secondary antibody-cocktail in TBS and 2% bovine serum albumin. After both antibody-incubations, every stained tissue was rinsed thoroughly with TBS, placed on protein glycerol–coated microscopic slides and mounted with Entellan® for proper examination of the results. Entellan® is a water-free mounting medium, containing toluene.[62]

Table 2: The cyanine fluorophores used in the methods and their excitation and emission peak wavelengths.

Cyanine fluorophore	Acronym	Excitation peak (nm)	Emission peak (nm)
Cyanine	Cy2	492	510
Indocarbocyanine	Cy3	550	570

The given values are only approximate and differ depending on the spectrofluorometer that is used.

3.1.1 Pre-treatment of tissue

The preserved tissue was treated with PBS (0,1 M, pH 7,4) for 10 minutes, following a 5-minute rinse in TBS (0,1 M, pH 7,4). After the rinse, Methanol (60%) was applied for 60 minutes. After stabilization, the tissue was incubated with TBS, 5% donkey-normal serum and 0,3% Triton X-100 for 45 minutes, to prevent unspecific binding.

3.1.2 DIFS of hAPP and parvalbumin

Since parvalbumin is found in 40% of all interneurons, parvalbumin antibodies detect the majority of these cells.[63] The primary antibody-cocktail was applied to the pre-treated tissue, containing rat anti-human APP (1:2) and rabbit anti-parvalbumin (1:2000) and

[62] "Entellan® 107960"

[63] Jorge J. Palop and Lennart Mucke: "Network abnormalities and interneuron dysfunction in Alzheimer disease"

incubated over night at 4°C. The next day, a secondary antibody-cocktail was incubated with the tissue for 60 minutes, targeting the primary antibodies. The cocktail contained Cy3 -conjugated donkey anti-rat (1:100) and Cy2 -conjugated donkey anti-rabbit (1:100).

3.1.3 DIFS of hAPP and calretinin

CR regulates other GABAergic inhibitory interneurons. Although it is one of the least abundant CaBPs in the brain, it could disclose CR -specific interneurons.[64] The tissue was treated with rabbit anti-calretinin (1:1000) and rat anti-human APP (1:2) and incubated over night at 4°C. After the incubation, Cy3 -conjugated donkey anti-rat (1:100) and Cy2 -conjugated donkey anti-rabbit (1:100) covered the tissue for an hour.

3.1.4 DIFS of hAPP and calbindin

Calbindin prevents flooding of neurons with glutamate, released from damaged neurons and is therefore an important marker for AD -research.[65] Rabbit anti-calbindin-D_{28k} (1:2000; the dilution of 1:1000 resulted in a high background signal) and rat anti-human APP (1:2) were applied to the tissue, which was then incubated over night at 4°C. The next day, the tissue was incubated with Cy3 -conjugated donkey anti-rat (1:100) and Cy2 -conjugated donkey anti-rabbit (1:100) for one hour.

3.1.5 DIFS of hAPP and somatostatin

Immunohistochemical stains of transgenic mouse-hippocampi with AD -pathology have shown a significantly reduced number of SST -positive interneurons compared to wildtype mouse tissue. Therefore, it was decided to use antibodies against SST, in order to examine the used tissue for this possible AD -pathologic characteristic.[66] The primary antibody-cocktail for this method contained rat anti-human APP (1:2) and goat anti-SST (1:100, the given dilution of 1:200 resulted in a not sufficiently stained tissue) and was incubated with the tissue over night at 4°C. The secondary antibody-cocktail consisted of Cy3 -conjugated donkey anti-rat (1:100) and Cy2 -conjugated donkey anti-goat (1:100).

---

[64] David Baglietto-Vargas et al.: “Calretinin interneurons are early targets of extracellular amyloid-beta pathology in PS1/AbetaPP Alzheimer mice hippocampus”

[65] Andressen C. et al: “Calcium-binding proteins: selective markers of nerve cells.”

[66] Yadong Huang and Lennart Mucke: “Alzheimer mechanisms and therapeutic strategies”

4 Results

The hippocampi of each fluorescently stained wildtype (WT) and transgenic (TG) tissue were photographed with BIOREVO BZ-9000, to gather enough data for a statistical evaluation of the immunohistochemical labellings. According to the cyanine-conjugated secondary antibody used in the individual labelling, a specific filter was used to photograph the hippocampi. Antibodies conjugated to Cyanine (Cy2), emit light in the green region of the visible spectrum, whereas those conjugated to Indocarbocyanine (Cy3) emit red light.

For the evaluation of possible colocalizations, the Keyence Corporation BZ-II Analyzer (version 2.2) was used to create an overlay of a green-fluorescent CaBP- or SST -marked transgenic tissue with the according red-fluorescent hAPP -labelling of the same tissue. With the same program, CaBP-, SST -positive and hAPP -expressing interneurons were counted and the number of interneurons containing both hAPP and a CaBP or SST was determined. The chapter 9 ‘appendices’ contains tables with all interneuron -numbers counted, which were analysed in the Results section.

Unfortunately, the number of interneurons located in the stratum pyramidale and stratum granulosum could only be estimated, because of the high cell density presented in these layers.

Table 3 contains necessary information about the transgenic mice of the type Tg2576, whose tissue was photographed.

Table 3: Age and ID of transgenic mice, whose tissue is displayed in the figures.

Method	**Figure**	**Identifier**	**Age**
hAPP/ Parvalbumin	8,9	Tg: #242 Wt: #545	Tg: 3 months Wt: 3 months
hAPP/ Calretinin	10,11	Tg:	Tg:

		#242 Wt: #545	3 months Wt: 3 months
hAPP/ Calbindin	12,13	Tg: #242 Wt: #544	Tg: 3 months Wt: 3 months
hAPP/ SST	15,16	Tg: #541 Wt: #545	Tg: 3 months Wt: 3 months

4.1 DIFS of hAPP and parvalbumin

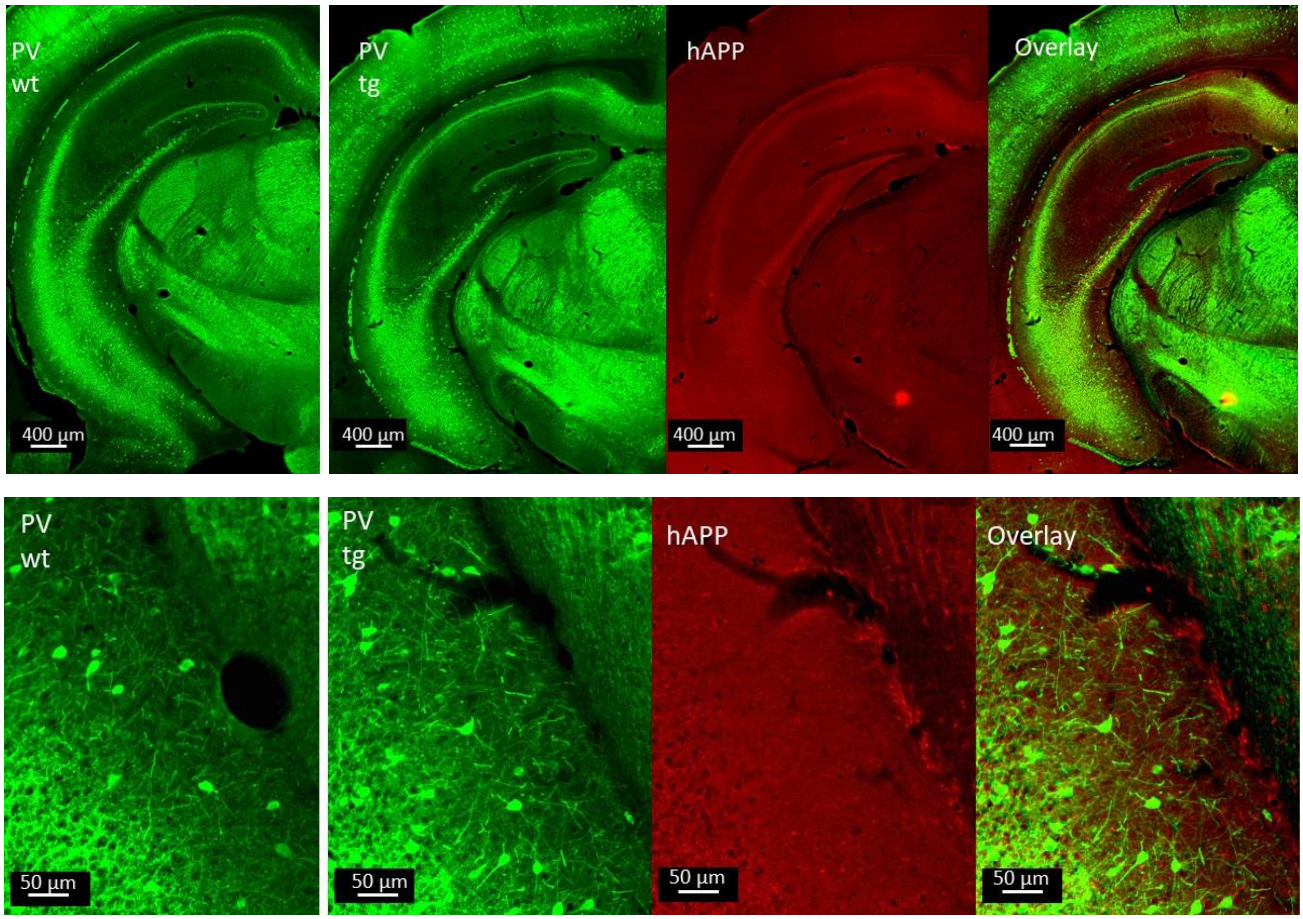

Figure 8: Overview of *PV -positive interneurons (green) and of hAPP -expressing interneurons (red) in wildtype and transgenic mouse hippocampus (top row). The bottom row shows higher magnification images of stained interneurons in the stratum oriens.*

The PV -stain of transgenic (TG) and wildtype (WT) -mice showed clear differences regarding the cell types of interneurons, which can be seen in figure 8. TG outnumbered the stained interneurons in the WT -tissue (for quantification see chapter 9.1, table 4). The WT -tissue showed the most PV -immunoreactivity in the stratum pyramidale, whereas the TG -mouse had the highest PV -occurrence in the subiculum. The highest hAPP -numbers were discovered in the stratum oriens. The cell density in the pyramidal layer, a part of which is shown in figure 8, affected the hAPP- and CaBP-/SST -count negatively in almost all stains regarding the identification of smaller and weakly stained neurons. Thus, the cell numbers in the pyramidal cell layers can only be estimated and are likely much higher than stated.

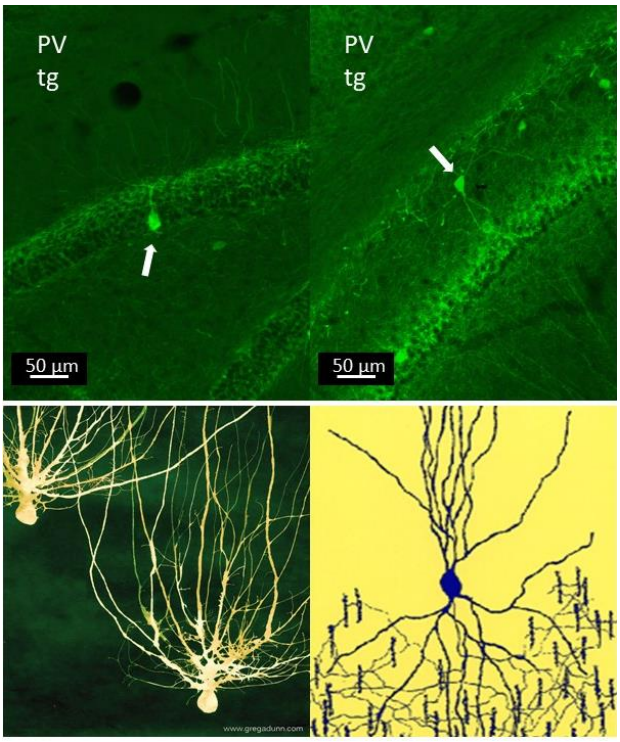

Figure 9: *The upper left picture shows a basket cell in the stratum granulosum of a TG -mouse immunoreactive for parvalbumin (PV). The upper right picture contains a chandelier cell, found in the stratum oriens of a TG mouse. The pictures underneath are general depictions of a basket cell (left; source: http://www.gregadunn.com/wp-content/uploads/2014/02/Basket-Cells.jpg; edited by: Emira Shehabi) and a chandelier cell (right; source: http://neuronbank.org/wiki/images/8/8e/Mine.jpg, edited by: Emira Shehabi). Status: 07.08.2017.*

In the stains, typically formed PV -positive interneurons were detected. A basket cell in the stratum granulosum in a TG mouse hippocampus with visible axons vertically projecting into the stratum moleculare, is demonstrated on the left picture of figure 9 (Top, arrow). A second type of typical PV -interneuron is the chandelier cell, which was found in the stratum oriens of a TG mouse hippocampus, projecting into the stratum pyramidale and stratum oriens. Both interneurons had a very clear form, visible axons and synaptic endings, which can be compared with the generalized pictures of such interneuron shapes in figure 9.

4.2 DIFS of hAPP and calretinin

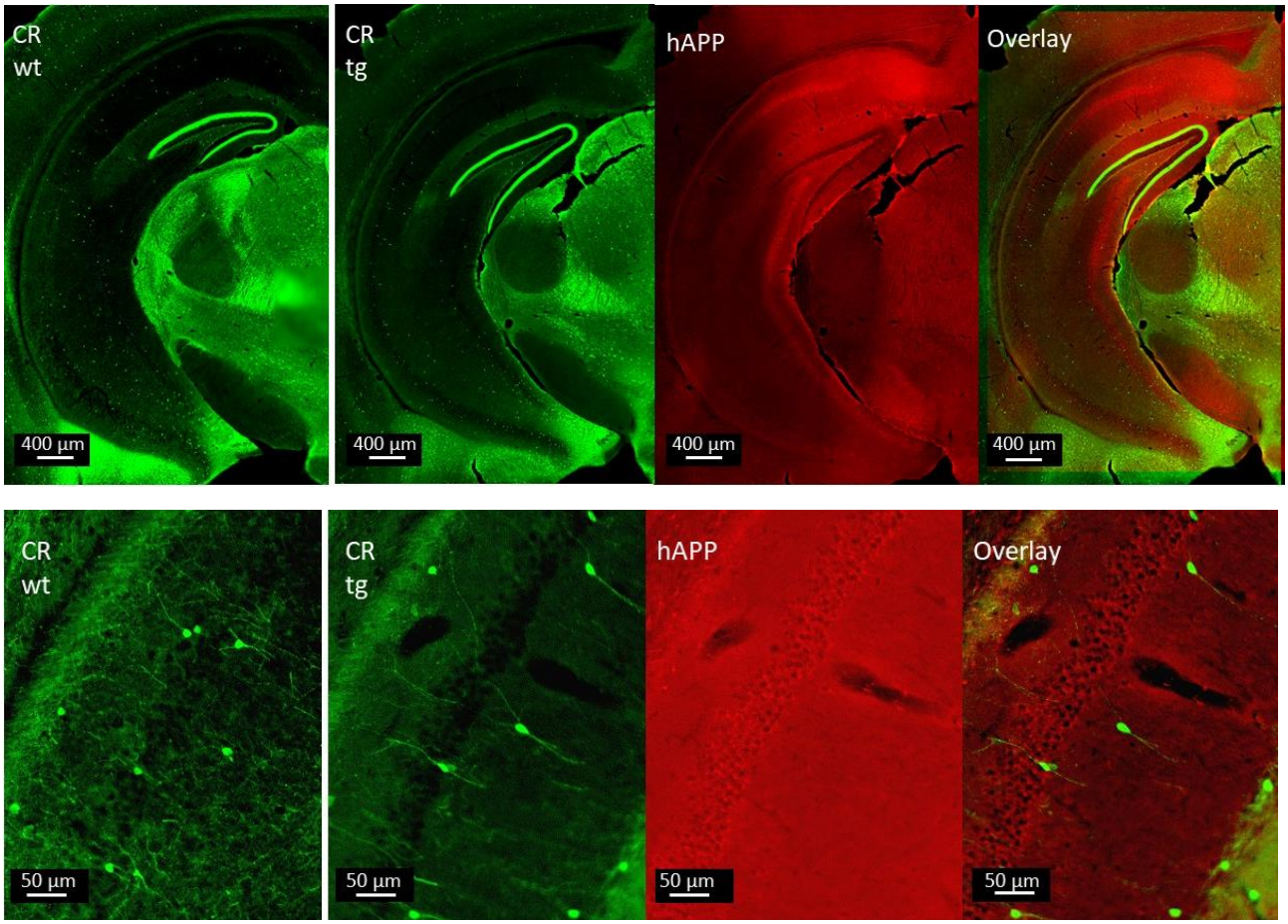

Figure 10: *Overview of CR -positive interneurons (green) and of hAPP -expressing interneurons (red) in wildtype and transgenic mouse. The bottom row shows higher magnification images of marked interneurons in the stratum oriens, stratum pyramidale and stratum radiatum.*

The CR -labelling demonstrated a similar outcome to the PV -immunohistochemistry regarding the number of marked interneurons, which was higher in TG (for quantification see chapter 9.1, table 5). As demonstrated in figure 10 (bottom row), the axons of the interneurons in the TG -tissue are more visible than in the WT mouse hippocampus. Again, the WT -tissue exhibited most marked interneurons in the stratum pyramidale and the TG -tissue in the subiculum. The highest hAPP -numbers could also be found in the stratum oriens.

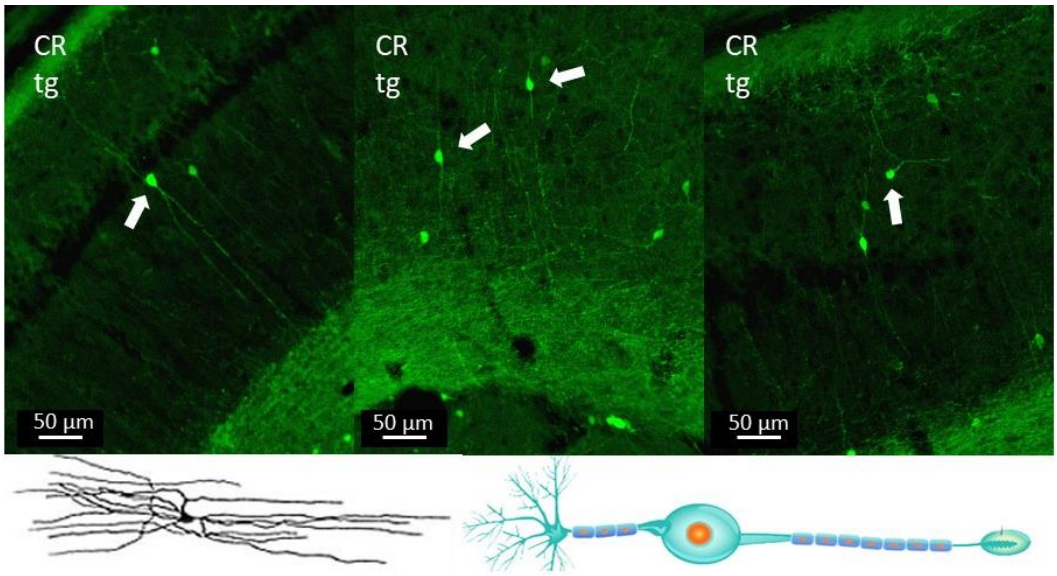

Figure 11: *The upper pictures show CR -typical interneurons in TG mouse hippocampi. From left to right: bitufted cell in the stratum radiatum, horizontal neuron in subiculum and basket-like cell in subiculum. The pictures underneath display a generalized picture of a bitufted (left; source: http://retina.umh.es/Webvision/imageswv/BasicCells.jpg; edited by: Emira Shehabi) and bipolar interneuron (right; source: http://media.buzzle.com/media/images-en/illustrations/human-biology/900-42870382-bipolar-neuron.jpg; edited by: Emira Shehabi). Status: 07.08.2017.*

One of the four CR -typical interneuron-types was not detected in the brain tissue analysed, which is the double bouquet cell. Finding certain interneurons in the tissue was not always an easy task, because of the different tissue qualities and differential descriptions of these interneurons, stated from various research groups. Although it is not certain, the CR -labelling in a tissue slice appears to have marked a bitufted cell in the stratum radiatum, whose axons are projecting into the stratum pyramidale and stratum lacunosum moleculare and can be seen on figure 11. Another, at first bipolar-appearing interneuron was found in the subiculum of a stain without any visible arborizations of the axon, which led to the assumption of it being a horizontal interneuron. An arborizing basket-like interneuron could also be found in the subiculum.

4.3 DIFS of hAPP and calbindin

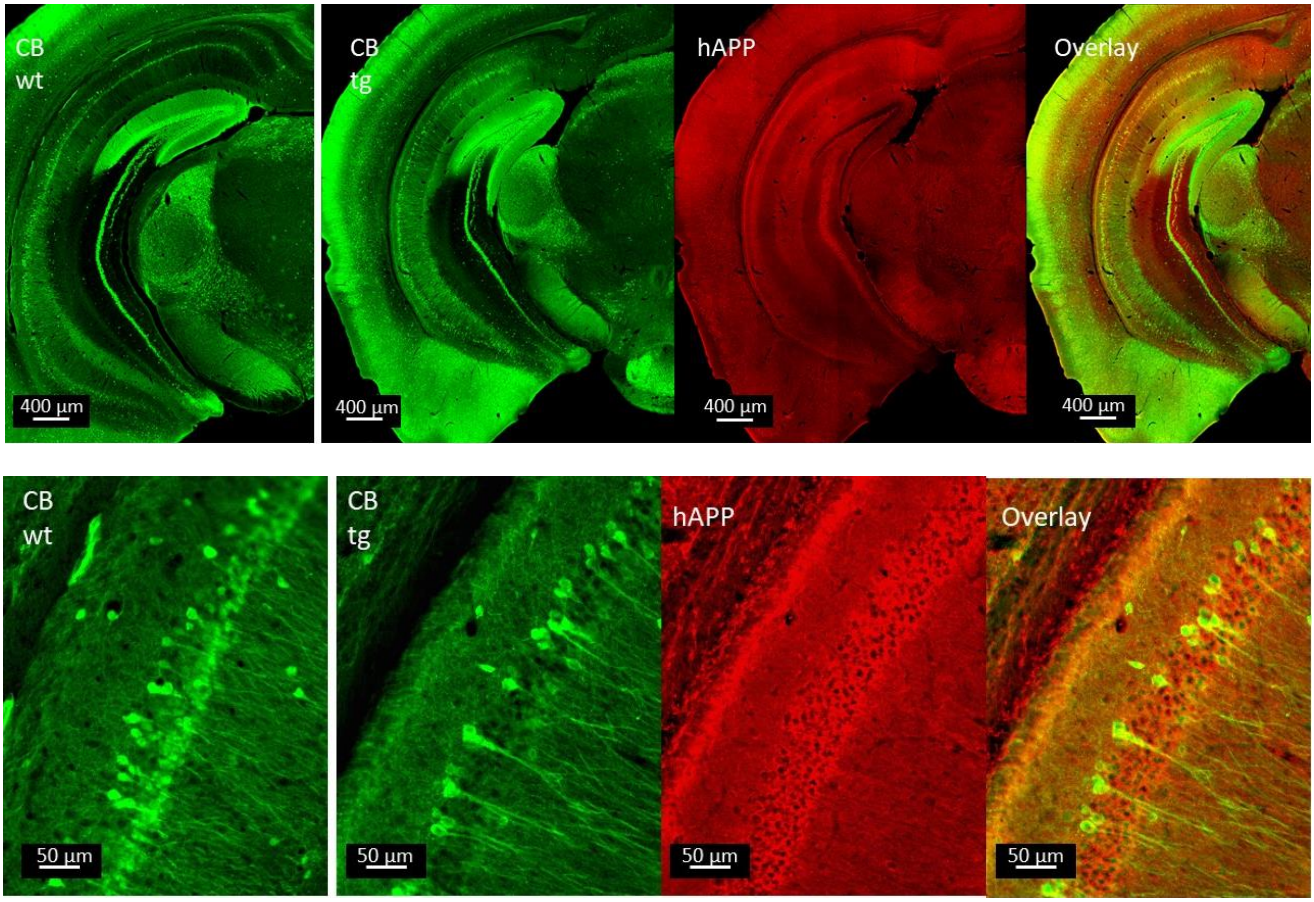

Figure 12: *Overview of CB -positive interneurons (green) and of hAPP -expressing interneurons (red) in wildtype and transgenic mouse. The bottom row shows higher magnification images of CB -stained interneurons in the stratum oriens, stratum pyramidale and stratum radiatum.*

In the TG -mouse tissue, the interneurons of the pyramidal cell layer demonstrated larger axonal projections into the stratum radiatum than in WT, which is shown in figure 12. These axonal projections of pyramidal interneurons were a characteristic of the CB -stain, represented in every marked tissue. The total number of CB -positive interneurons was surprisingly much higher in TG (for quantification see chapter 9.1, table 6). The highest interneuron-numbers were found in the stratum oriens in the WT and the stratum pyramidale of the TG -tissue. The highest hAPP -occurrence was seen in the stratum pyramidale.

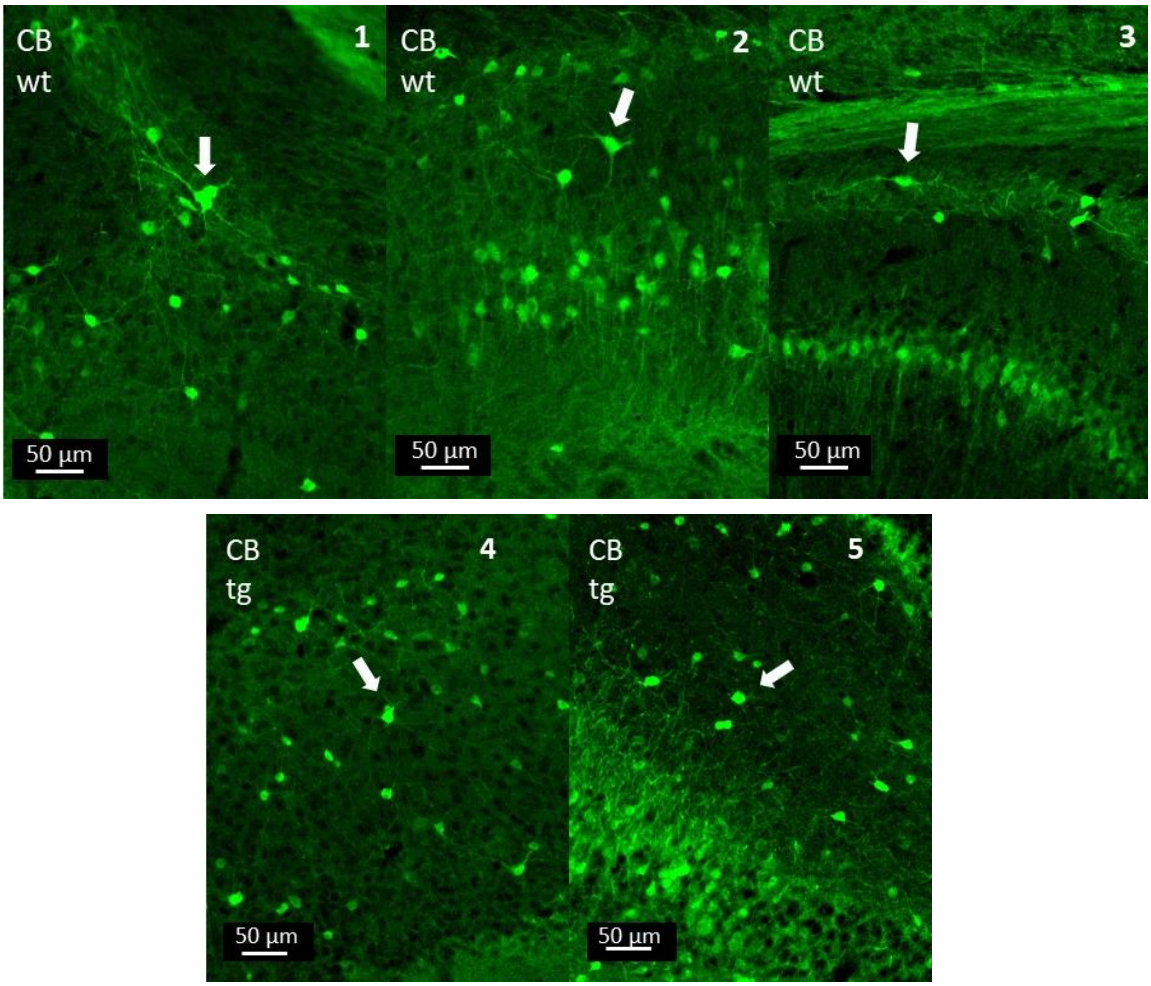

Figure 13: *A high number of typically formed, CB -expressing interneurons could be found in both TG- (bottom row) and WT -tissue (top row). Top row: 1. Double bouquet cell in subiculum. 2. Chandelier cell in subiculum. 3. Horizontal cell in stratum oriens. Bottom row: 4. Chandelier-looking cell in subiculum. 5.Bitufted-looking cell in stratum radiatum.*

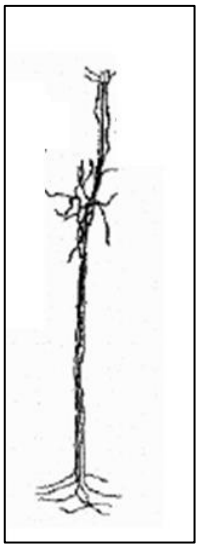

Figure 14: *Depiction of a double bouquet cell. Source: http://www.genesis-sim.org/GENESIS/Tutorials/genesis-intro/tutfigs/cortical_cells4.gif; edited by: Emira Shehabi. Status: 14.08.2017.*

Calbindin is expressed in several types of interneurons, some of which could be discovered here, as seen on figure 13. In picture 5 of figure 13, a possibly bitufted interneuron was detected in the stratum radiatum of a Tg2576 hippocampus. Because of the several axons, it could also represent a chandelier cell. The same case is depicted in picture 4, showing either a bitufted or chandelier cell (because of an edgy appearance of the cell body) in the subiculum of a TG -tissue. A double bouquet cell was found in the subiculum of a WT -stain (picture 1) and is characterized by several arborizations on the ends of its axons, which are weakly stained. It can be compared with the generalized picture of a double bouquet cell in figure 14. A typical chandelier cell in the subiculum of a WT -stain can be viewed in picture 2. It owns a clear form with an edgy cell body and axons arranged in a triangular, chandelier-like way with several axons projecting horizontally into the stratum radiatum and only one axon vertically into the stratum pyramidale. Lastly, a horizontal interneuron or double bouquet cell can be seen in picture 3, which is located in the stratum oriens of a calbindin labelling. Because of visible axonal arborizations and a similarity to the interneuron in picture 1, it is more likely to be a double bouquet cell. The interneuron types that were not found were the bitufted and the basket cell, the latter of which is typically expressed in the pyramidal layer, which is very fluorescent in the stain and thus complicated the search. Noticeable were the clear forms

of interneurons in the WT -tissue, which affected the identification of CB -typical interneurons very positively.

4.4 DIFS of hAPP and somatostatin

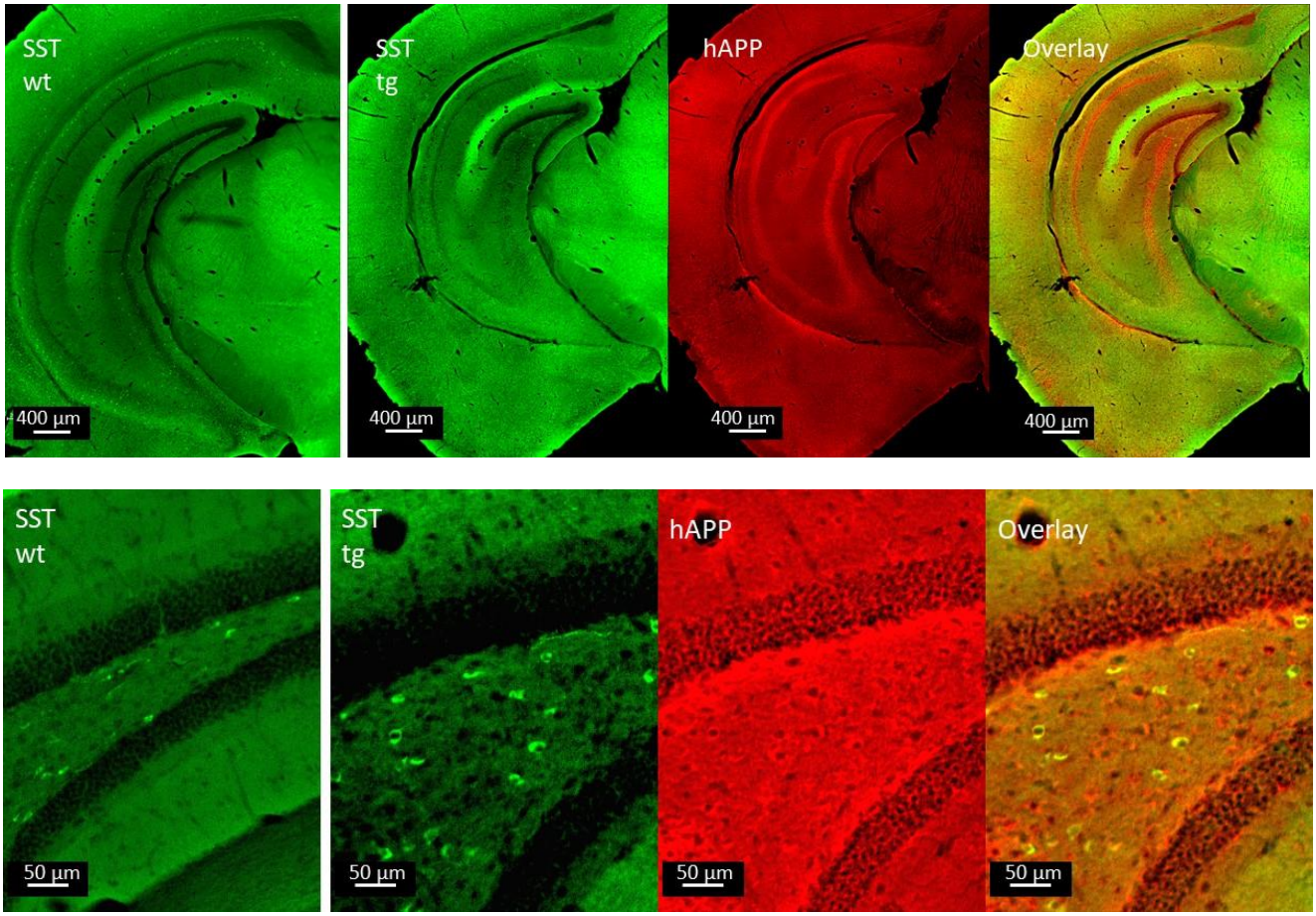

Figure 15: *Overview of SST -positive interneurons (green) and of hAPP -expressing interneurons (red) in wildtype and transgenic mouse. The bottom row shows higher magnification images of interneurons in the DG -area.*

The SST -labelling showed a decrease in compound-levels in the transgenic animal (for quantification see chapter 9.1, table table 7). As seen on figure 15 (bottom row), the interneurons of TG and WT -tissue exhibited big cell nuclei. The most interneurons could be found in the stratum oriens of the WT and TG -mouse tissue. The highest hAPP -numbers were seen in the stratum oriens, closely followed by the subiculum.

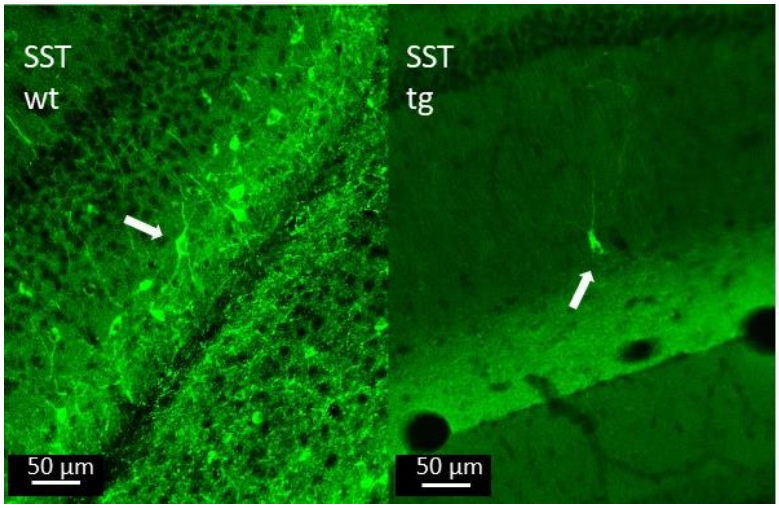

Figure 16: *In the WT -tissue on the left picture, a martinotti-like cell was discovered. On the right picture, a basket cell-like interneuron was found in TG -tissue.*

A possibly basket-like interneuron with a large cell nucleus could be found in a TG -tissue in the stratum radiatum, whereas in the stratum oriens of a WT -stain a martinotti type of cell was discovered, with several axons spiking out of its cell body and several arborizations of its axons. Both cell types can be seen in figure 16. SST is typically expressed in martinotti cells and thus should be included in SST -stains.

4.5 Quantitative comparison of CaBP- and SST -positive interneurons in transgenic mice and wildtype mice

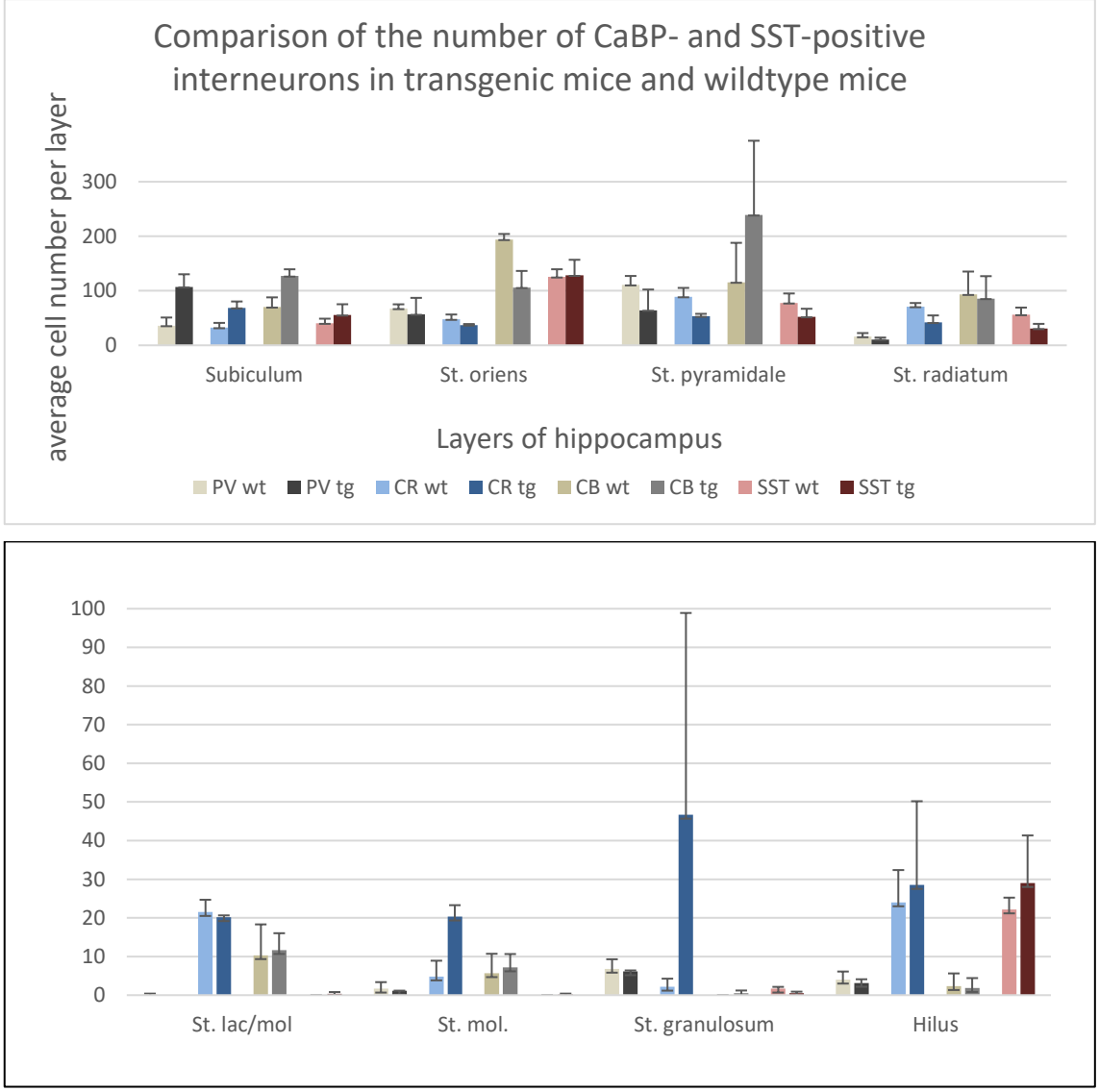

Figure 17: *A statistical comparison of the number of CaBP- and SST -positive interneurons in TG and WT, in hippocampal layers. The numbers are demonstrated in two diagrams, because of very low interneuron-numbers in the strata lacunosum moleculare, moleculare, granulosum and the hilus. These strata are represented in the second diagram.*

The Cy2 -marked interneurons, expressing the CaBPs PV, CR and CB and the neuropeptide SST were counted in 8 regions of both hippocampi in the brains of WT and TG -mice. Additionally, Cy3 -marked, hAPP -expressing interneurons were counted in the hippocampi of TG -mice. Interneurons co-expressing hAPP and CaBPs or the neuropeptide SST in the stained tissue were quantified by exact overlaying of the green

Cy2- and red Cy3 -labelling of the same tissue. The obtained interneuron-numbers were averaged and used for further statistical analyses.

First, potential differences in the numbers of CaBP- and SST -expressing neurons between WT and TG -mouse tissue were analysed. The numbers are presented in two diagrams because the interneuron-number in some hippocampal layers was rather low and did not fit the y-scale. The statistic evaluation of the counted CaBP- or SST -labelled interneurons in all TG and WT -tissues analysed, revealed only for the SST -labelling more interneurons in the WT -tissue than in TG hippocampus, with an averaged number of 323±42 SST -positive interneurons. Surprisingly, all CaBP -positive interneurons were found at higher numbers in the TG mouse hippocampus.

As demonstrated in figure 17, calbindin was the CaBP expressed at the highest numbers out of all CaBPs and neuropeptides. In both WT and TG hippocampus, CB was detected in numbers near and over 100, especially in the subiculum (WT: 70±18; TG: 218±12), stratum oriens (WT: 194±10; TG: 106±30), stratum pyramidale (WT: 116±72; TG: 239±136) and stratum radiatum (WT: 93±42; TG: 159±41). CR was especially dominant in the stratum pyramidale (89±16) and stratum radiatum (71±7) in WT and in the subiculum (69±12) and stratum pyramidale (53±5) in TG. PV only occurred in high numbers in the subiculum (107±23) and stratum pyramidale (64±38) in TG and in the stratum pyramidale (111±16) and stratum oriens (67±8) in WT. SST had a high occurrence in the stratum oriens (WT: 125±14; TG: 128±29) and the hilus (WT: 22±3; TG: 29±12) in both mouse genotypes, the latter of which is known to contain many interneurons with SST -like immunoreactivity. In addition, it was found that the three CaBPs were the most prominent in the stratum pyramidale and the neuropeptide SST had its strongest occurrence in the stratum oriens in both TG and WT.

4.6 Comparison of CaBP-, SST- and hAPP -expressing interneuron-numbers in the wildtype and transgenic hippocampus

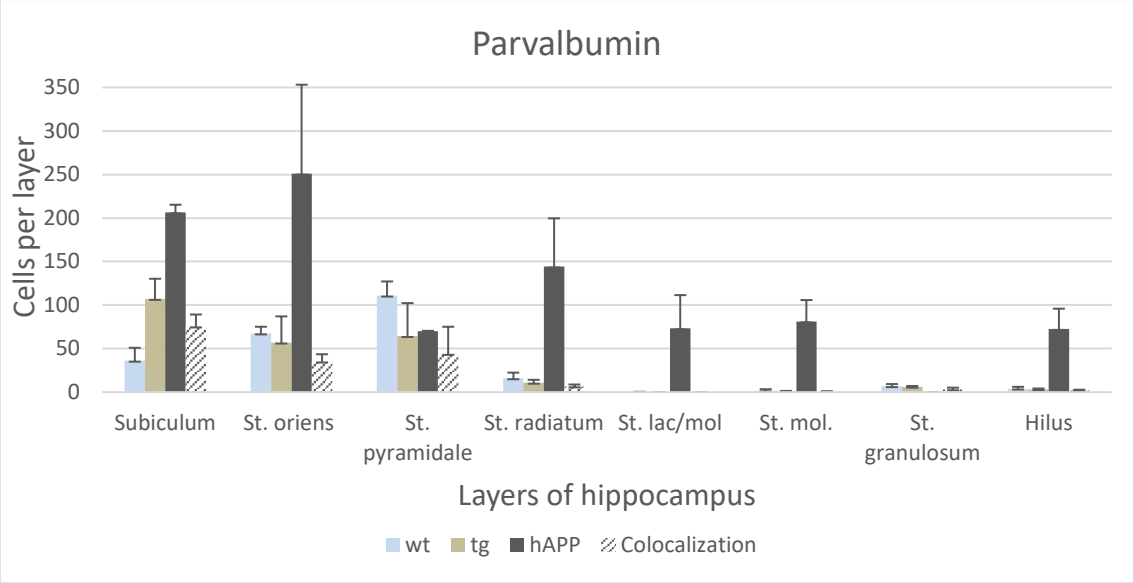

Figure 18: *Comparison of the numbers of PV -positive neurons in WT and TG mouse hippocampus with hAPP -expressing interneurons and colocalization of PV and hAPP.*

Second, a comparison of the numbers of CaBP-, SST- and hAPP -expressing interneurons in the wildtype and transgenic hippocampus tissue, with an additional comparison of the neuronal numbers coexpressing both proteins, was made.

PV -expressing interneurons were found in the highest quantity in the subiculum of the TG -mouse tissue (107±23; all numbers are given in chapter 9.1, table 4) and the stratum pyramidale (111±16) of the WT -mouse tissue, whereas almost no PV -labelling was found in the stratum lacunosum moleculare, the stratum moleculare, stratum granulosum and the hilus for both TG and WT mice. Summing up all hippocampal layers, the transgenic tissue contained more PV neurons (249±37) than WT (243±36). The highest number of neurons expressing the hAPP transgene was found in stratum oriens (251±102) and the subiculum (206±9). The highest number of neurons coexpressing hAPP and PV was found in the subiculum (75±14), followed by the stratum pyramidale (44±31).

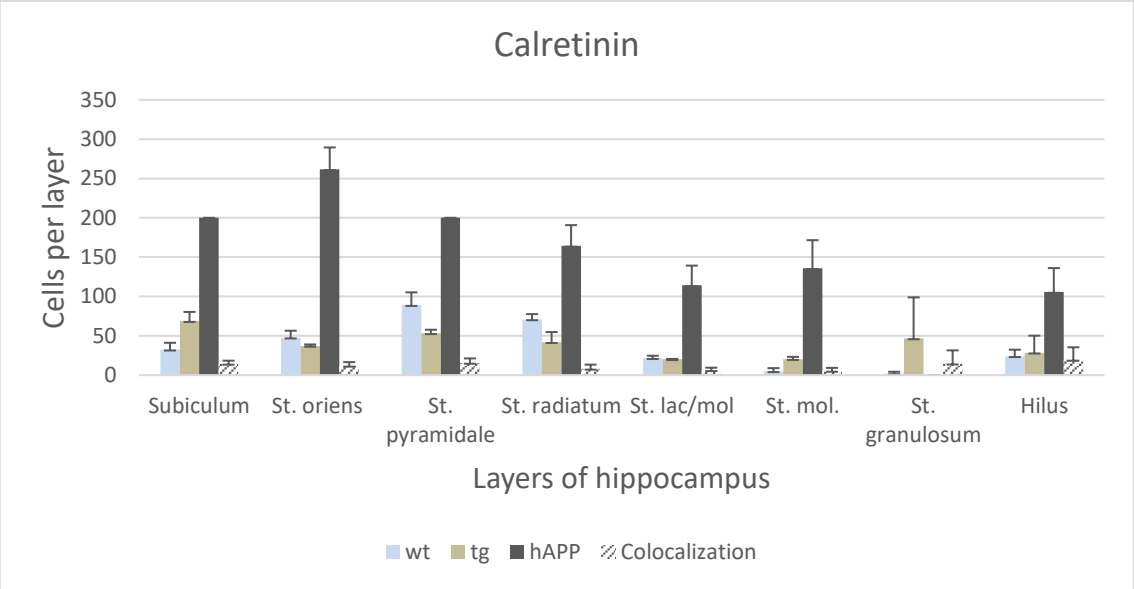

Figure 19: *Comparison of the numbers of CR -positive neurons in WT and TG mouse hippocampus with hAPP -expressing interneurons and colocalization of CR and hAPP.*

Compared to the PV -labelling, there were more CR -immunoreactive neurons in every layer of the hippocampus. The highest quantity of CR -positive interneurons was found in the subiculum of the TG -tissue (69±12; all numbers are given in chapter 9.1, table 5) and the stratum pyramidale (89±16) of the WT. More CR -positive neurons were found in the transgenic tissue (317±16) than in the WT -tissue (292±29). The highest hAPP -occurrence was found in stratum oriens (262±28) and the stratum pyramidale and subiculum with an estimated number of 200 each, which is likely much higher due to its high cell density. Colocalizations of hAPP and CR were found especially in the hilus (19±16) and followed by the stratum pyramidale (16±6).

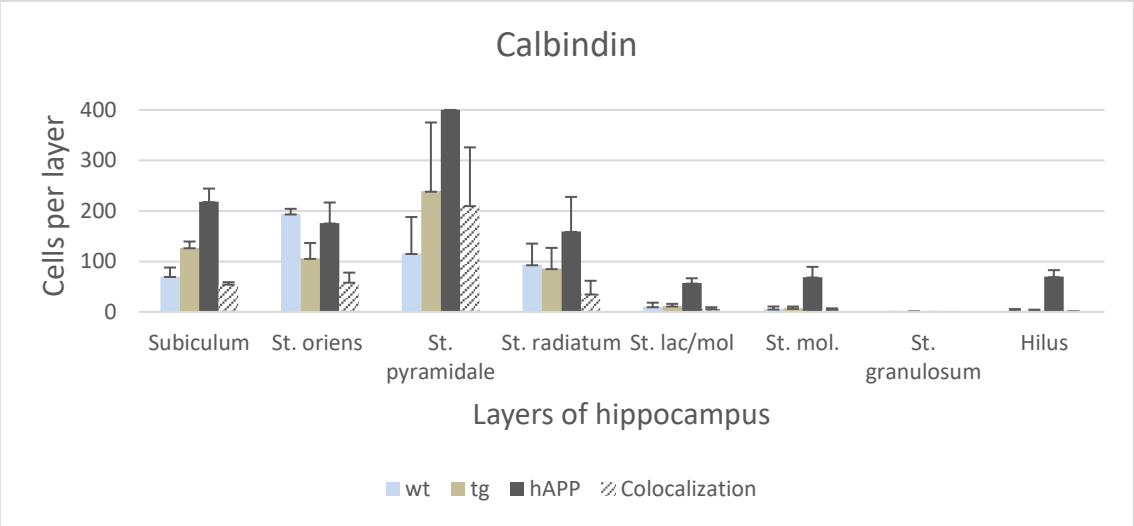

Figure 20: *Comparison of the numbers of CB -positive neurons in WT and TG mouse hippocampus with hAPP -expressing interneurons and colocalization of CB and hAPP.*

The highest numbers of neurons labelled for CaBPs were detected by the CB immunohistochemistry with total numbers in the TG stratum pyramidale of 239±136 (all numbers are given in chapter 9.1, table 6) and the stratum oriens of WT (194±10). The transgenic mice showed a much higher number of CB (579±79) than WT (492±66). The highest hAPP -concentration was found in the stratum pyramidale with an estimated number of 400 (which is likely much higher) and the subiculum (218±26). CB was found to be mostly colocalized with hAPP in the stratum pyramidale (211±115) and stratum oriens (59±19), the first of which indicates the highest colocalization-number out of all CaBPs and neuropeptides tested in this project.

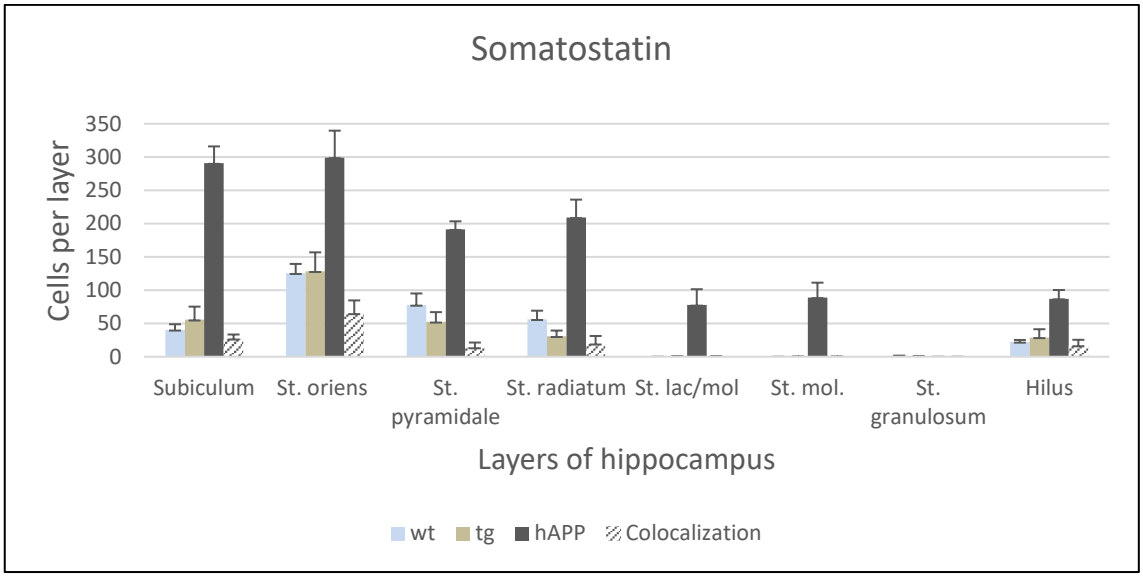

Figure 21: *Comparison of the numbers of SST -positive neurons in WT and TG mouse hippocampus with hAPP -expressing interneurons and colocalization of SST and hAPP.*

In comparison to the CaBPs, the neuropeptide SST was expressed by fewer neurons, except in the stratum oriens, where relatively high numbers of neurons positive for SST were found. Stratum lacunosum moleculare, stratum moleculare and the stratum granulosum showed almost no SST -immunoreactivity. As mentioned, the highest occurrence of SST was found in the stratum oriens of TG (128±29) and WT (125±14) mice (all numbers are given in chapter 9.1, table 7). More SST -positive neurons were discovered in the WT (323±42) than in TG (297±40) and therefore it marked the first and only compound in the project that showed less interneurons in TG. The hAPP was found to be mostly expressed in stratum oriens (299±40) and the subiculum (291±25). Since hAPP and SST were found mostly in stratum oriens and the subiculum, the most colocalizations occurred in these layers (stratum oriens: 65±20; subiculum: 27±7).

4.7 Ratio of CaBP-, SST- and hAPP -positive interneurons to average hAPP -positive interneuron-number of all stains per hippocampal layer

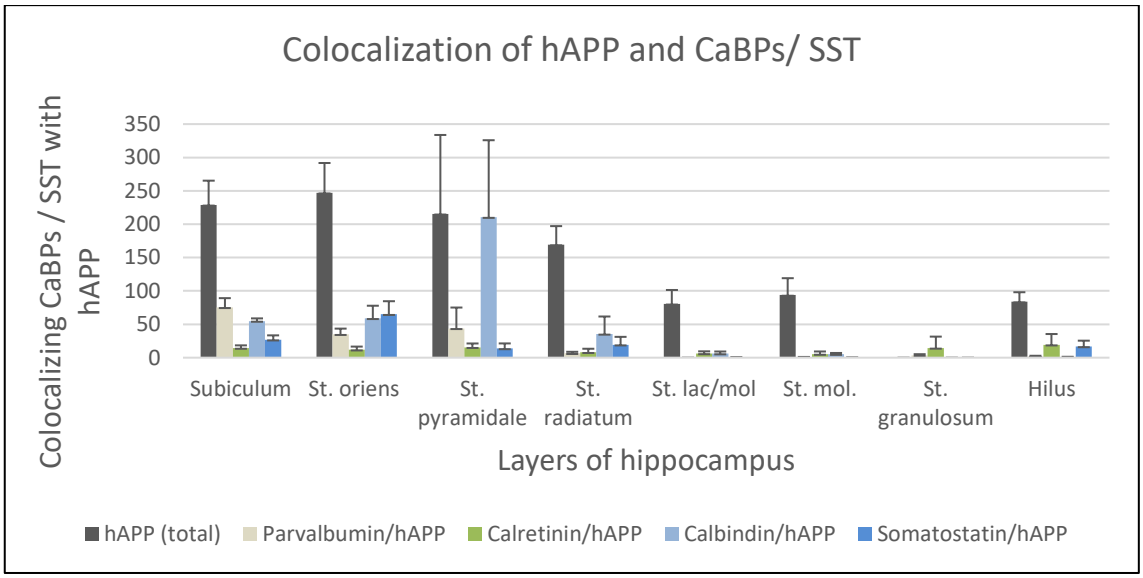

Figure 22: *This diagram demonstrates the total, average hAPP -numbers per layer in all performed stains and the average colocalization-rates of the CaBPs/ SST with hAPP per layer.*

Next, the average numbers of interneurons per layer, co-expressing hAPP and CaBPs/ SST were compared to the hAPP -numbers that have been averaged for every layer in all stains (CB, PV, CR, SST) to examine the colocalization-rates. As previously mentioned, the highest numbers of neurons coexpressing CaBPs and hAPP were detected for CB in the stratum pyramidale (table 12). In this layer, an average number of 215±118 hAPP -positive neurons was calculated and 211±115 CB- and hAPP -positive interneurons were counted. In the subiculum, PV had the second highest degree of colocalization with hAPP of 75±14 PV- and hAPP -positive interneurons and 229±36 hAPP -expressing interneurons. In the same layer, CB reached a colocalization-number of 55±4, marking CB as the second most colocalizing compound in this layer. The stratum oriens contained a very high number of 247±45 hAPP -positive interneurons and 65±20 SST- and hAPP -expressing interneurons. In the stratum radiatum, CB was again the compound with the highest colocalization of 36±26. In the other layers, the number of hAPP -positive interneurons was much higher than the colocalization of CaBPs/SST. The strata lacunosum moleculare, moleculare, granulosum and the hilus delivered only a low number of CaBP-/SST -positive interneurons, but even in the stratum lacunosum

moleculare and the stratum moleculare mostly CB, closely after CR, was colocalizing with hAPP.

4.8 Comparison of CaBP- or SST- and hAPP -positive interneurons in all layers of the hippocampus

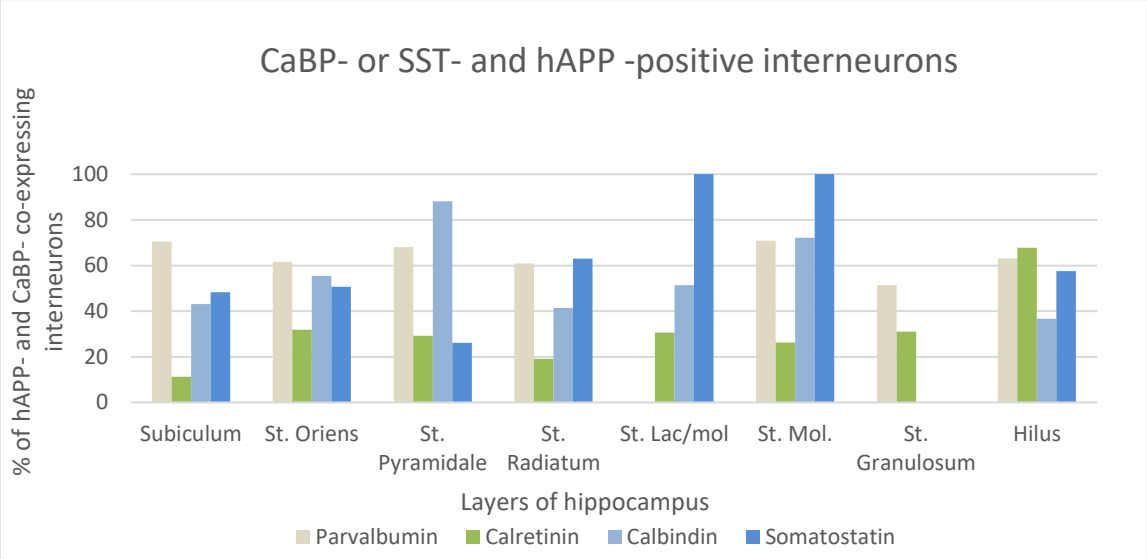

Figure 23: *This statistical evaluation states the percentages of colocalizing CaBPs/ SST with hAPP per averaged, total CaBP-/ SST-number in the same hippocampal layer.*

The percentage of colocalizing CaBPs/SST to the total CaBP-/SST -count in every layer was calculated to reveal how many counted CaBPs/SST were simultaneously colocalized with hAPP. In almost every layer, except for the stratum lacunosum moleculare and stratum moleculare, over 50% of PV was colocalized with hAPP (all numbers are given in chapter 9.4, table 13). The subiculum contained the highest percentage of colocalizing PV with 70%. In the strata oriens, pyramidale, lacunosum moleculare and moleculare over 50% of CB was found to be colocalizing with hAPP. The stratum pyramidale contained 88% and the stratum moleculare 72% of CB. Remarkably, every SST -positive interneuron in the stratum lacunosum moleculare was noticed to colocalize with every marked hAPP -expressing interneuron. Additionally, 63% of SST was colocalized with hAPP in the stratum radiatum. Only in the hilus, CR was found to be the most colocalized compound with over 68%.

5 Discussion

The aim of this project was to analyse the cell type-specific coexpression of the hAPP transgene by CaBP -expressing interneurons in the hippocampus in the Tg2576 mouse model of AD. To address this issue, hippocampal brain sections of three, three-month-old hAPP -transgenic (TG) Tg2576 mice and three wildtype (WT) mice were treated with antibodies against the CaBPs parvalbumin, calretinin, calbindin and the neuropeptide somatostatin. The hAPP -expressing interneurons were marked with antibodies in the transgenic tissue concurrently, to calculate absolute numbers and proportions of hippocampal interneurons coexpressing hAPP and the respective CaBP or the neuropeptide SST.

The hippocampal layers of WT and TG -tissue with the highest occurrences of CaBPs, SST and hAPP found in this project were the stratum oriens, stratum pyramidale and the subiculum. In the WT -tissue alone, most interneurons were found in the stratum pyramidale of the PV- and CR -labelling and the stratum oriens of the CB- and SST -stain. The TG -tissue showed the highest numbers of interneurons in the subiculum of the PV- and CR -labelling, the stratum pyramidale of the CB -stain and the stratum oriens of the SST -labelling. The highest hAPP -numbers of both WT and TG -mice tissue were found in the stratum oriens of the PV-, CR- and the SST -labelling, as well as the stratum pyramidale of the CB -stained tissue.

The WT reflects the naturally occurring neuronal numbers in a given brain structure without any inserted, possibly neuron-damaging genetic mutation, like the AD -mutation in Tg2576 -mice that accumulates AD -like plaques in the brain and leads to reduced neuronal numbers in clinical AD. Therefore, it was expected to also find a higher number of CaBPs and SST in the murine WT than TG -tissue, which was thought to exhibit much less CaBP- and SST -positive interneurons. Surprisingly, the only protein that was found in higher numbers in the marked WT -hippocampi was SST. This is the only result of this project, that partly correlates with the findings about clinical AD, which report reduced neuronal numbers of CaBP- and neuropeptide-expressing interneurons and therefore

higher numbers in patients without AD. [67,68,69] Regarding the occurrence in hippocampal layers, the labelling showed much higher numbers in the hilus of TG- and WT -hippocampus than CB and PV and contained high numbers of SST -expressing interneurons in the stratum oriens in the TG -tissue and in the stratum pyramidale of the WT hippocampal tissue. These strata are generally known to contain the highest density of SST neurons, together with the hilus. However, almost no SST -immunoreactivity was found in the stratum moleculare and stratum granulosum of the DG, which corresponds with the reports of Sloviter et al., that also found a rather rare occurrence of SST in these two layers.[70]

Inhibitory, GABAergic interneurons have been found to comprise around 11% of the total neuron population in the hippocampus.[71] Previous studies have described PV -immunoreactive interneurons to form 32-38% of these GABAergic interneuron-population in the hippocampus.[72] Interestingly, in this project PV appeared to be distributed in high quantities only in the stratum pyramidale and oriens in the WT -mice and the subiculum and stratum pyramidale in the TG -mice with a total number of 243±36 in the WT and 249±37 in the TG -mice. However, the numbers of PV -positive interneurons in these layers were highly outnumbered by the CB -marked tissue, which showed a much higher immunoreactivity in the same layers in both TG- and WT -labellings.

[67] Jean-Pierre et al. Brion: “A subset of calretinin-positive neurons are abnormal in Alzheimer's disease”

[68] Harald Stefanits, Carolin Wesseling and Gabor G. Kovacs: “Loss of Calbindin immunoreactivity in the dentate gyrus distinguishes Alzheimer's disease from other neurodegenerative dementias”

[69] “Parvalbumin-immunoreactive neurons in the hippocampal formation of Alzheimer's diseased brain - ScienceDirect”

[70] RS. Sloviter and G. Nilaver: “Immunocytochemical localization of GABA-, cholecystokinin-, vasoactive intestinal polypeptide-, and somatostatin-like immunoreactivity in the area … - PubMed - NCBI”

[71] Godavarthi S. et al: “Reversal of reduced parvalbumin neurons in hippocampus and amygdala of Angelman syndrome model mice by chronic treatment of fluoxetine - Godavarthi - 2014 - Journal of Neurochemistry - Wiley Online Library”

[72] Ibid.

Previously, CB has been reported to occur in only 10-20% of GABAergic interneurons, located in the hippocampus.[73] However, in this project CB was found to be the most abundantly occurring protein in TG- and WT -mice in almost all layers out of all the marked CaBPs and neuropeptides with a total average of 492±66 marked CB -positive interneurons in the WT and 579±79 in the TG -mouse. In only 3 of the 8 examined hippocampus layers, which were the stratum oriens, stratum radiatum and hilus, the WT -mouse had a higher number of CB -positive neurons than the TG -mouse. The obtained average hAPP -numbers of the CB -stained tissue slices were the second highest after CR, and CB was found to colocalize with hAPP in many more layers in higher numbers than the other CaBPs. The reason for the higher number of CB -expressing interneurons in the transgenic tissue is unclear, because there are no obvious reasons for this result, such as bad quality of WT -tissue and therefore a lower amount of marked CaBPs. Consecutive brain sections from the same WT- and TG -tissue were used in all methods to ensure the analyses of identical brain structures with comparable neuronal densities. Furthermore, mice analysed were of the same age.

In regard to other studies with CaBPs, the numbers obtained in this project could be the result of a weak primary antibody against PV, which can be assumed because of a similar problem during the labelling of CB and CR. Since the CB- and CR -labelling resulted in very weakly stained tissue, it was decided to perform the same stain with newly ordered primary antibodies against CB and CR, which succeeded in binding more CaBPs and therefore produced an intense stain of the tissue. Indeed, the new antibody against CR and CB marked much more interneurons than the antibody against PV and resulted in the highest CaBP -positive interneuron numbers that were obtained in both WT- and TG -tissue. Although CR -positive interneurons have been reported to only form about 13% of all GABAergic interneurons in the hippocampus, the CR -labelling in this project marked the second highest CaBP -number in tested WT- and TG -mice.[74] The labelling of PV didn't show any weakly stained PV -positive interneurons, but the obtained PV -numbers were too low, when compared to the numbers of CB- and CR -labelled

[73] Ibid.

[74] Dhiraj Maskey et al.: "Changes in the distribution of calbindin D28-k, parvalbumin, and calretinin in the hippocampus of the circling mouse"

interneurons, since PV should be distributed in higher concentrations among the hippocampus.

Nonetheless, a malfunctioning primary antibody against PV doesn't explain the high colocalization of CB with hAPP, which was observed in this project. The obtained colocalization-numbers could indicate a protecting mechanism by CB against A-β, which was discovered by Moon et al. The researchers used three-months-old tissue from a different transgenic mouse line (5XFAD) with 5 AD -mutations, which was incubated with mouse anti-human A-β and antibodies against CaBPs and A-β. The results showed no plaques in the regions containing CB -expressing interneurons and let the researchers conclude, that CB can hinder A-β -accumulation in interneurons and therefore the formation of plaques.[75] If these results are applicable to all CB -immunoreactive interneurons in transgenic mouse hippocampi and especially the Tg2576 -mouse line, the high CaBP- and colocalization-numbers of the CB -labelling in this project could provide further evidence for a protecting mechanism by CB against A-β.

Because of insufficient evidence, it is not exactly known if CaBPs generally have an ability to suppress APP -processing and the generation of A-β or if only the accumulation into plaques can be prevented.[76] The study didn't mention any analysed colocalizations of CB and hAPP, which could have explained if CB can colocalize with a certain level of hAPP, concurrently hindering the accumulation of more into plaques. Therefore, it is unclear if the CB in this project, that was found to colocalize with hAPP, would have hindered the accumulation of more A-β into plaques or if the results of the mentioned study are only applicable to the 5XFAD -mouse type and the obtained CB -numbers of this project would have reduced with increasing age and initiating A-β deposits in the tested transgenic mice.

[75] Minho Moon et al.: "Intracellular amyloid-β accumulation in calcium-binding protein-deficient neurons leads to amyloid-β plaque formation in animal model of Alzheimer's disease"

[76] Ibid.

In clinical AD, parvalbumin-, calretinin- and calbindin-levels were proven to decrease with higher APP -levels. [77,78,79] Some research has shown, that high APP -concentrations can be related with reduced CaBP -numbers in transgenic mice with the hAPP -transgene as well, but a number of other studies have stated the opposite and therefore the exact molecular relationship between hAPP and CaBPs in transgenic mice is not known.[80]
In aged humans and certain animals, A–β has been shown to be affected by Ca^{2+} -ions and concurrently be able to influence the influx of these ions, which has an impact on CaBPs. In experiments, "a spectrum of A*β* impact, from complete disintegration of the […] bilayer phase to modest perturbations in bilayer structure and enhanced permeability of [Ca^{2+}-] ions" [81] was discovered by Lockhart et al. These disordering effects strengthen with deeper embedding of A-β into the membrane and increases the calcium-influx into the area, elevating the local concentration of ions by over 25% because of the strong binding affinity of calcium towards negatively charged amino acids and thus A-β. Ca^{2+} -ions have a minor impact on A-β secondary structure, but a much higher influence on the tertiary structure by disrupting several intramolecular long-range interactions in the peptide. Increased intra- and extracellular calcium-concentrations in the brain have been shown to correlate with decreased CB- and CR -levels, accelerating the growth of A-β -aggregates and the formation of plaques.[82] Because of this evidence, a calcium influx-reducing compound has been given to moderate and severe AD -patients, which has shown to improve cognition.[83]

[77] Jean-Pierre et al. Brion: "A subset of calretinin-positive neurons are abnormal in Alzheimer's disease"

[78] Harald Stefanits, Carolin Wesseling and Gabor G. Kovacs: "Loss of Calbindin immunoreactivity in the dentate gyrus distinguishes Alzheimer's disease from other neurodegenerative dementias"

[79] "Parvalbumin-immunoreactive neurons in the hippocampal formation of Alzheimer's diseased brain - ScienceDirect"

[80] Ibid.

[81] C. Lockhart and D. Klimov: "Calcium Enhances Binding of Aβ Monomer to DMPC Lipid Bilayer"

[82] Ibid.

[83] American Society for Biochemistry and Molecular Biology: "Acceleration of Amyloid β-Peptide Aggregation by Physiological Concentrations of Calcium"

Generally, interneurons expressing CaBPs are known to have the ability of buffering intracellular calcium in humans and rodents, which otherwise may cause excitotoxicity.[84] Hence, if the function of CaBPs is to buffer Ca^{2+} -concentrations intracellularly, the decreased CB- and CR -levels in the experiment of Lockhart et al. had to be caused by abnormally high Ca^{2+} -levels in the neurons that couldn't be buffered by the CaBPs, or a very high calcium-concentration in the extracellular space, since there is no mentioning about the ability of CaBPs to buffer Ca^{2+} extracellularly.

Regarding the results in this project, it is possible that the study of Lockhart et al. is not applicable to Tg2576 mice and the inserted hAPP -gene in the Tg2576 mouse does not react with Ca^{2+} -ions in the same way as in human AD -patients or other animals with the hAPP -transgene, since the CR- and CB -levels were not reduced. It could indicate a differential interaction by A-β with membranes and lipid bilayers in the Tg2576 mouse, which could have little to no impact on Ca^{2+} -ions and CaBPs. A study of Kalback et al. has indeed found significant chemical and physical differences of A-β -deposits in the brains of Tg2576 mice, which could include a different impact of hAPP on Ca^{2+} -ions.[85] Therefore, if the hAPP -transgene in the Tg2576 -mouse doesn't increase Ca^{2+} -concentrations and CaBPs are rather affected (and decreased) by abnormally increased Ca^{2+} -influx than A-β -levels, the high numbers of CaBPs and colocalizing compounds in the TG -tissue of this project are logical. Unfortunately, this would discredit Tg2576 as a reliable AD -model, even though insertion of the hAPP -gene into these mice does initiate accumulation of A-β into plaques.

Another possibility for the outcome of this project, is that the initial CaBP -concentration was higher in the tested transgenic animals and the developed number of A-β didn't have much effect on CaBP -levels yet, because of the young age of tested mice (3 months). By early analysis, the possibility of decreased CaBP -levels with increasing age and A-β -deposits couldn't be explored. Various stress factors during the transport and storage of the transgenic and wildtype animals could also be reasons for the abnormal CaBP -concentrations or the lower SST -level in the WT -mice.

[84] C. E. Ribak, R. Nitsch and L. Seress: "Proportion of parvalbumin-positive basket cells in the GABAergic innervation of pyramidal and granule cells of the rat hippocampal formation"

[85] Kalback W et al.: "APP transgenic mice Tg2576 accumulate Abeta peptides that are distinct from the chemically modified and insoluble peptides deposited in Alzheimer's disease senile plaques"

In conclusion, the obtained data in this project was rather unexpected, since PV-, CB- and CR -levels have all been found to decrease or at least abnormally develop in the brains of human AD -patients.[86,87,88] If neuronal loss is a major characteristic of clinical AD and this and other studies, e.g. by researchers such as Irizzary et al. resulted in 'little to no loss of neurons in Tg2576 mice'[89], this transgenic mouse line should be used with caution and regard to controversial studies. If the goal is to gather information about clinical AD, which can be used for further evaluation, only those transgenic animal models should be used, that are known to display typical neuronal changes, as seen in the clinical disease.

[86] Jean-Pierre et al. Brion: "A subset of calretinin-positive neurons are abnormal in Alzheimer's disease"

[87] Harald Stefanits, Carolin Wesseling and Gabor G. Kovacs: "Loss of Calbindin immunoreactivity in the dentate gyrus distinguishes Alzheimer's disease from other neurodegenerative dementias"

[88] "Parvalbumin-immunoreactive neurons in the hippocampal formation of Alzheimer's diseased brain - ScienceDirect"

[89] Jennifer Horgan et al.: "Longitudinal brain corticotropin releasing factor and somatostatin in a transgenic mouse (TG2576) model of Alzheimer's disease"

6 Outlook

Because of unexpected data, which was obtained during the statistical evaluation of the labellings and gathered evidence of the Tg2576 mouse line being a rather unreliable model for clinical AD, it should be considered to use another animal model or transgenic mouse line, which is known to show typical symptoms of clinical AD. Besides the mouse line, other factors can be changed for a better evaluation and more reliable results. First, animals of increasing age groups should be chosen in order to evaluate how hAPP -concentrations change with increasing age. This kind of statistical data would have answered the question, if the stained mouse-tissue was too young to show a decrease in CaBPs. Certainly, it is also possible to use older mice with already formed A-β -plaques and high A-β -levels, since these mice should show a significant decrease in CaBP -levels, according to clinical AD -neuropathology. Because of the higher lipofuscin-number in the tissue of older mice, which has the unfortunate property of intensifying the background signal of immunohistochemical labellings, this method would complicate statistical evaluation. Therefore, it is rather suggested to perform the immunohistochemical staining on increasing age groups of 3-, 6- and 8-months-old tissue in order to avoid high lipofuscin-levels but still gather enough information on changes of hAPP– and CaBP -numbers with increasing age. Another improvement could be provided through a counting software, which is able to exactly detect interneurons in hippocampal layers, such as the stratum pyramidale and stratum granulosum. As mentioned, these layers often contained a high number of stained interneurons which was too high to be counted manually or CaBP- and SST -immunoreactive interneurons were not exactly distinguishable from other pyramidal or granular neurons, that weren't marked. The obtainment of an exact interneuron-number in these two layers would immensely benefit the comparison of CaBP– and especially hAPP -numbers, which were found to be very high in the stratum pyramidale. Another problem occurred during the analysis of many labellings, because of a too intensely stained stratum pyramidale and, regarding the CB -labelling, a too fluorescent DG -area. Here, it should be experimented with the utilized volume of primary and secondary antibodies to assure a sufficient, but weaker stain. Finally, the employed antibodies must function normally, in order to gather comparable data. Because of a possibly malfunctioning primary antibody against PV, the obtained

data of the labelling was rather surprising when compared to the other CaBPs, for which new primary antibodies were ordered shortly before immunohistochemical staining.

Lastly, it should be considered to not only analyse AD on a microscopic level, but also focus on the macroscopic aspect -or on the human himself. How does the average person, in parts of the world that have high AD -rates, spend his day and what are factors, still unknown to the average human that could trigger a neurodegenerative disease? Evidence of AD being a primarily vascular disease has been already published back in 1907 by Stelzmann et al., who has observed arteriosclerotic changes in post-mortem tissue of AD -patients.[90] Researchers at the 39th Annual Williamsberg Conference on Heart Disease even explained, how easily atherosclerosis is produced experimentally in herbivores "by giving them diets containing large quantities of cholesterol (egg yolks) or saturated fat (animal fat)". [91] Such a diet can additionally cause hypoperfusion by increasingly clogged arteries in the whole body, which has also been associated with AD.[92] Although many confusions exist regarding the best diet for humans, an herbivorous or plant-based diet is described as very beneficial for humans of every age in many studies. A plant-based diet has even been shown to reverse diseases, like diabetes, cancer and vascular diseases.[93,94,95,96,97] These findings indicate that most of western diseases, including AD, can be provoked with an inappropriate diet. Research should therefore set its focus on prevention of these diseases by elucidation of known risk factors which are included in

[90] R. et al.A Stelzmann: "An English translation of Alzheimer's 1907 paper, "Uber eine eigenartige Erkankung der Hirnrinde". - PubMed - NCBI"

[91] Mina M. Benjamin and William C. Roberts: "Facts and principles learned at the 39th Annual Williamsburg Conference on Heart Disease"

[92] Benjamin P. Austin et al.: "Effects of hypoperfusion in Alzheimer's disease"

[93] B. et al. Caldwell: "A way to reverse CAD?"

[94] Tai Le, L. et al.: "Beyond Meatless, the Health Effects of Vegan Diets: Findings from the Adventist Cohorts"

[95] Mina M. Benjamin and William C. Roberts: "Facts and principles learned at the 39th Annual Williamsburg Conference on Heart Disease"

[96] M. et al. Glick-Bauer: "The Health Advantage of a Vegan Diet: Exploring the Gut Microbiota Connection"

[97] American Dietetic Association: "Position of the American Dietetic Association"

the daily routine, especially the diet of an average human, living in parts of the world that are highly affected by AD and co.

7 Bibliography

Alzheimer Forschung Initiative e.V. “Zahlen und Fakten der Alzheimer-Krankheit in Deutschland.” Accessed April 28, 2017. https://www.alzheimer-forschung.de/alzheimer-krankheit/faktenblatt_zahlen.htm.

American Dietetic Association. “Position of the American Dietetic Association: Vegetarian Diets.” *Journal of the American Dietetic Association* 109, no. 7 (2009): 1266–82. doi:10.1016/j.jada.2009.05.027.

American Society for Biochemistry and Molecular Biology. “Acceleration of Amyloid β-Peptide Aggregation by Physiological Concentrations of Calcium.” Accessed July 17, 2017. http://www.jbc.org/content/281/38/27916.full.

Andressen C. et al. “Calcium-binding proteins: selective markers of nerve cells.” Accessed April 30, 2017. https://www.ncbi.nlm.nih.gov/pubmed/8453652.

Austin, Benjamin P., Veena A. Nair, Timothy B. Meier, Guofan Xu, Howard A. Rowley, Cynthia M. Carlsson, Sterling C. Johnson, and Vivek Prabhakaran. “Effects of hypoperfusion in Alzheimer's disease.” *Journal of Alzheimer's disease JAD* 26 Suppl 3 (2011): 123–33. Accessed August 16, 2017. doi:10.3233/JAD-2011-0010. https://www.ncbi.nlm.nih.gov/pmc/articles/PMC3303148/pdf/nihms356990.pdf.

Baglietto-Vargas, David, Ines Moreno-Gonzalez, Raquel Sanchez-Varo, Sebastian Jimenez, Laura Trujillo-Estrada, Elisabeth Sanchez-Mejias, and Manuel Torres et al. “Calretinin interneurons are early targets of extracellular amyloid-beta pathology in PS1/AbetaPP Alzheimer mice hippocampus.” *Journal of Alzheimer's disease JAD* 21, no. 1 (2010): 119–32. Accessed May 9, 2017. doi:10.3233/JAD-2010-100066. http://content.iospress.com/download/journal-of-alzheimers-disease/jad100066?id=journal-of-alzheimers-disease%2Fjad100066.

Benjamin, Mina M., and William C. Roberts. “Facts and principles learned at the 39th Annual Williamsburg Conference on Heart Disease.” Accessed August 16, 2017. https://www.ncbi.nlm.nih.gov/pmc/articles/PMC3603726/pdf/bumc0026-0124.pdf.

Brion, Jean-Pierre e. a. “A subset of calretinin-positive neurons are abnormal in Alzheimer's disease.” Accessed August 13, 2017. https://www.researchgate.net/publication/15257208_A_subset_of_calretinin-positive_neurons_are_abnormal_in_Alzheimer%27s_disease.

Bywalez, and Wolfgang. “Physiology of rodent olfactory bulb interneurons.” Accessed July 14, 2017. https://edoc.ub.uni-muenchen.de/19836/index.html.

Caldwell, B. e. a. “A way to reverse CAD?” Accessed August 22, 2017. http://dresselstyn.com/JFP_06307_Article1.pdf.

David Hubel. “Eye, Brain, and Vision.” Accessed April 30, 2017. http://hubel.med.harvard.edu/book/b1.htm.

Duvernoy, Henri M., Françoise Cattin, and Pierre-Yves Risold. *"The Human Hippocampus": "Functional Anatomy, Vascularization and Serial Sections with MRI"*. 4th ed. 2013. Dordrecht: Springer, 2013.

“Entellan® 107960.” Accessed April 21, 2017. http://www.sigmaaldrich.com/catalog/product/mm/107960?lang=de&region=DE.

Glick-Bauer, M. e. a. “The Health Advantage of a Vegan Diet: Exploring the Gut Microbiota Connection.” Accessed August 22, 2017. https://www.ncbi.nlm.nih.gov/pmc/articles/PMC4245565/.

Godavarthi S. et al. “Reversal of reduced parvalbumin neurons in hippocampus and amygdala of Angelman syndrome model mice by chronic treatment of fluoxetine - Godavarthi - 2014 - Journal of Neurochemistry - Wiley Online Library.” Accessed August 21, 2017. http://onlinelibrary.wiley.com/doi/10.1111/jnc.12726/full.

Heather Caroline Rice. “Selective Vulnerability of Interneurons in Alzheimer’s Disease.” Accessed March 27, 2017. http://www.alz.org/research/alzheimers_grants/for_researchers/overview-2016.asp?grants=2016rice.

Höfling, Corinna, Markus Morawski, Ulrike Zeitschel, Elisa R. Zanier, Katrin Moschke, Alperen Serdaroglu, and Fabio Canneva et al. “Differential transgene expression patterns in Alzheimer mouse models revealed by novel human amyloid precursor protein-specific antibodies.” *Aging cell* 15, no. 5 (2016): 953–63. doi:10.1111/acel.12508.

Horgan, Jennifer, Jose J. Miguel-Hidalgo, Martha Thrasher, and Garth Bissette. “Longitudinal brain corticotropin releasing factor and somatostatin in a transgenic mouse (TG2576) model of Alzheimer's disease.” *Journal of Alzheimer's disease JAD* 12, no. 2 (2007): 115–27.

Huang, Yadong, and Lennart Mucke. “Alzheimer mechanisms and therapeutic strategies.” *Cell* 148, no. 6 (2012): 1204–22. doi:10.1016/j.cell.2012.02.040.

Kandalepas, Patty C., and Robert Vassar. “The Normal and Pathologic Roles of the Alzheimer's β-secretase, BACE1.” *Current Alzheimer research* 11, no. 5 (2014): 441–49.

Kelsom, Corey, and Wange Lu. “Development and specification of GABAergic cortical interneurons.” *Cell & Bioscience* 3, no. 1 (2013): 19. doi:10.1186/2045-3701-3-19. https://cellandbioscience.biomedcentral.com/track/pdf/10.1186/2045-3701-3-19?site=cellandbioscience.biomedcentral.com.

Knowing Neurons. “Inhibitory Neurons: Keeping the Brain’s Traffic in Check.” Accessed April 18, 2017. http://knowingneurons.com/2014/11/05/inhibitory-neurons-keeping-the-brains-traffic-in-check/.

Koch, Christof, and R. C. Reid. “Neuroscience: Observatories of the mind.” *Nature* 483, no. 7390 (2012): 397–98. doi:10.1038/483397a.

Learn.Genetics. “The Other Brain Cells.” Accessed April 13, 2017. http://learn.genetics.utah.edu/content/neuroscience/braincells/.

Lockhart, C., and D. Klimov. “Calcium Enhances Binding of Aβ Monomer to DMPC Lipid Bilayer.” Accessed July 17, 2017. http://www.cell.com/biophysj/fulltext/S0006-3495(15)00228-3.

M, Joanna, K. Stachowicz, G. Nowak, and A. Pilc. “The Loss of Glutamate-GABA Harmony in Anxiety Disorders.” In *Anxiety disorders*. Edited by Vladimir Kalinin. Rijeka: InTech, 2011.

Markram, Henry, Maria Toledo-Rodriguez, Yun Wang, Anirudh Gupta, Gilad Silberberg, and Caizhi Wu. “Interneurons of the neocortical inhibitory system.” *Nature reviews. Neuroscience* 5, no. 10 (2004): 793–807. doi:10.1038/nrn1519.

Maskey, Dhiraj, Jonu Pradhan, Cheol K. Oh, and Myeung J. Kim. “Changes in the distribution of calbindin D28-k, parvalbumin, and calretinin in the hippocampus of the circling mouse.” *Brain research* 1437 (2012): 58–68. Accessed August 21, 2017. doi:10.1016/j.brainres.2011.12.009. http://cyber.sci-hub.cc/MTAuMTAxNi9qLmJyYWlucmVzLjIwMTEuMTIuMDA5/maskey2012.pdf.

Mayer, Joanne, Michelle G. Hamel, and Paul E. Gottschall. “Evidence for proteolytic cleavage of brevican by the ADAMTSs in the dentate gyrus after excitotoxic lesion of the mouse entorhinal cortex.” *BMC neuroscience* 6 (2005): 52. doi:10.1186/1471-2202-6-52.

Mayfield Clinic. “Anatomy of the Human Brain.” Accessed April 30, 2017. https://www.mayfieldclinic.com/PE-AnatBrain.htm.

MedlinePlus Medical Encyclopedia. “Lipofuscin.” Accessed May 1, 2017. https://medlineplus.gov/ency/article/002242.htm.

Moon, Minho, Hyun-Seok Hong, Dong W. Nam, Sung H. Baik, Hyundong Song, Sun-Young Kook, Yong S. Kim, Jeewoo Lee, and Inhee Mook-Jung. “Intracellular amyloid-β accumulation in calcium-binding protein-deficient neurons leads to amyloid-β plaque formation in animal model of Alzheimer's disease.” *Journal of Alzheimer's disease JAD* 29, no. 3 (2012): 615–28. Accessed July 17, 2017. doi:10.3233/JAD-2011-111778.

Noemí Bronstein-Sitton. “Somatostatin and the Somatostatin Receptors: Versatile Regulators of Biological Activity.” *Pathways*, no. 2 (2006). Accessed May 9, 2017. http://www.alomone.com/upload/newsletters/pathways%202%20papers/somatostatin%20and%20the%20somatostatin%20receptors%20versatile%20regulators%20of%20biological%20activity.pdf.

OLSEN, RICHARD W. “GABA.” Accessed April 18, 2017.

Palop, Jorge J., and Lennart Mucke. “Network abnormalities and interneuron dysfunction in Alzheimer disease.” *Nature Reviews Neuroscience* 17, no. 12 (2016): 777–92. Accessed March 27, 2017. doi:10.1038/nrn.2016.141.

“Parvalbumin-immunoreactive neurons in the hippocampal formation of Alzheimer's diseased brain - ScienceDirect.” Accessed August 13, 2017. http://www.sciencedirect.com/science/article/pii/S0306452297000687.

Pesold, C., W. S. Liu, A. Guidotti, E. Costa, and H. J. Caruncho. “Cortical bitufted, horizontal, and Martinotti cells preferentially express and secrete reelin into perineuronal nets, nonsynaptically modulating gene expression.” *Proceedings of the National Academy of Sciences* 96, no. 6 (1999): 3217–22. Accessed July 31, 2017. doi:10.1073/pnas.96.6.3217.

Ribak, C. E., R. Nitsch, and L. Seress. “Proportion of parvalbumin-positive basket cells in the GABAergic innervation of pyramidal and granule cells of the rat hippocampal formation.” *The Journal of comparative neurology* 300, no. 4 (1990): 449–61. Accessed August 21, 2017. doi:10.1002/cne.903000402.

Rice University. “Hippocampus.” Accessed April 28, 2017. http://www.caam.rice.edu/~cox/wrap/hippocampus.pdf.

Schmid, Lena C., Manuel Mittag, Stefanie Poll, Julia Steffen, Jens Wagner, Hans-Rüdiger Geis, and Inna Schwarz et al. “Dysfunction of Somatostatin-Positive Interneurons Associated with Memory Deficits in an Alzheimer’s Disease Model.” *Neuron* 92, no. 1 (2016): 114–25. doi:10.1016/j.neuron.2016.08.034.

Scientific American Blog Network. “Know Your Neurons: How to Classify Different Types of Neurons in the Brain's Forest.” Accessed July 16, 2017. https://blogs.scientificamerican.com/brainwaves/know-your-neurons-classifying-the-many-types-of-cells-in-the-neuron-forest/.

Sloviter, RS., and G. Nilaver. “Immunocytochemical localization of GABA-, cholecystokinin-, vasoactive intestinal polypeptide-, and somatostatin-like immunoreactivity in the area … - PubMed - NCBI.” Accessed June 28, 2017. https://www.ncbi.nlm.nih.gov/pubmed/3819038.

Snellman, Anniina, Francisco R. Lopez-Picon, Johanna Rokka, Mario Salmona, Gianluigi Forloni, Mika Scheinin, Olof Solin, Juha O. Rinne, and Merja Haaparanta-Solin. “Longitudinal amyloid imaging in mouse brain with 11C-PIB: comparison of APP23, Tg2576, and APPswe-PS1dE9 mouse models of Alzheimer disease.” *Journal of nuclear medicine official publication, Society of Nuclear Medicine* 54, no. 8 (2013): 1434–41. doi:10.2967/jnumed.112.110163.

Statista - Universität Leipzig. “Statistiken zur weltweiten Verbreitung von Demenz.” Accessed April 28, 2017. https://de.statista.com/themen/2032/demenzerkrankungen-weltweit/.

Stefanits, Harald, Carolin Wesseling, and Gabor G. Kovacs. “Loss of Calbindin immunoreactivity in the dentate gyrus distinguishes Alzheimer's disease from other neurodegenerative dementias.” *Neuroscience letters* 566 (2014): 137–41. doi:10.1016/j.neulet.2014.02.026.

Stelzmann, R. e. a.A. “An English translation of Alzheimer's 1907 paper, "Uber eine eigenartige Erkankung der Hirnrinde". - PubMed - NCBI.” Accessed August 16, 2017. https://www.ncbi.nlm.nih.gov/pubmed/8713166.

Tai Le, L. et al. “Beyond Meatless, the Health Effects of Vegan Diets: Findings from the Adventist Cohorts.” Accessed August 22, 2017. https://www.ncbi.nlm.nih.gov/pmc/articles/PMC4073139/.

Team, PhysiologyWeb. “Physiological Significance of the Membrane Potential: Resting Membrane Potential.” Accessed April 28, 2017. http://www.physiologyweb.com/lecture_notes/resting_membrane_potential/resting_membrane_potential_physiological_significance_of_the_membrane_potential.html.

Terai, K., A. Iwai, S. Kawabata, Y. Tasaki, T. Watanabe, K. Miyata, and T. Yamaguchi. “beta-amyloid deposits in transgenic mice expressing human beta-amyloid precursor protein have… - Abstract - Europe PMC.” Accessed August 13, 2017. http://europepmc.org/abstract/MED/11377835.

U.S. National Library Of Medicine. “PSEN1 gene: presenilin 1.” Accessed April 30, 2017. https://ghr.nlm.nih.gov/gene/PSEN1#conditions.

Vassar, Robert, Dora M. Kovacs, Riqiang Yan, and Philip C. Wong. “The beta-secretase enzyme BACE in health and Alzheimer's disease: regulation, cell biology, function, and therapeutic potential.” *The Journal of neuroscience the official journal of the Society for Neuroscience* 29, no. 41 (2009): 12787–94. doi:10.1523/JNEUROSCI.3657-09.2009.

W, Kalback, Watson MD, Kokjohn TA, Kuo YM, Weiss N, Luehrs DC, and Lopez J et al. “APP transgenic mice Tg2576 accumulate Abeta peptides that are distinct from the chemically modified and insoluble peptides deposited in Alzheimer's disease senile plaques.” *Biochemistry* 41, no. 3 (2002): 922–28. doi:10.1021/bi015685.

Yang, Juan, Song Li, Xi-Biao He, Cheng Cheng, and Weidong Le. “Induced pluripotent stem cells in Alzheimer's disease: applications for disease modeling and cell-replacement therapy.” *Molecular neurodegeneration* 11 (2016). doi:10.1186/s13024-016-0106-3.

8 Bibliography of figures

Figure 1: ‘The main sections of the brain’. URL: http://www.nova.org.au/sites/default/files/images/people-and-medicine/brain/brain-illustrations-02-v6_670x449.png [28.04.2017].

Figure 2: ‘The components of the limbic system’. URL: http://classconnection.s3.amazonaws.com/252/flashcards/1048252/png/forebrain1328987872235.png. [28.04.17].

Figure 3: ‘Comparison of the human and mouse brain’. URL: http://www.getdomainvids.com/rdg.html? [Stand: 15.08.2017].

Figure 4: ‘The layers of the hippocampus in mice’. URL: http://anatomie.vetmed.uni-leipzig.de/external/hippocampus/index.html [Stand: 28.04.2017].

Figure 5: ‘Synthesis of glutamate and GABA in glutamatergic and GABAergic neurons’. URL: https://oatext.com/img/Glutamate-transporters-1.jpg [Stand: 28.04.2017].

Figure 6: ‘The structure of an interneuron and of a sensory neuron’. URL: http://www.biologymad.com/nervoussystem/relayneurone.jpg*;* http://classtalkers.com/wp-content/uploads/2011/11/structure_of_a_neurone1.jpg [Stand: 24.08.2017].

Figure 9: ‘General depictions of a basket cell and a chandelier cell’. URL: http://www.gregadunn.com/wp-content/uploads/2014/02/Basket-Cells.jpg***;*** http://neuronbank.org/wiki/images/8/8e/Mine.jpg [Status: 07.08.2017].

Figure 11: ‘Generalized picture of a bitufte and bipolar interneuron’. URL: http://retina.umh.es/Webvision/imageswv/BasicCells.jpg; http://media.buzzle.com/media/images-en/illustrations/human-biology/900-42870382-bipolar-neuron.jpg [Status: 07.08.2017].

Figure 14: ‘Depiction of a double bouquet cell’. URL: http://www.genesis-sim.org/GENESIS/Tutorials/genesis-intro/tutfigs/cortical_cells4.gif [Status: 14.08.2017].

9 Appendices

9.1 Quantitative comparison of CaBP- and SST-positive interneurons in transgenic mice and wildtype mice

Table 4: Quantitative comparison of PV-positive interneurons in transgenic mice and wildtype mice

PV	Subiculum	St. oriens	St. pyramidale	St. radiatum	St. lac/mol	St. mol	St. granulosum	Hilus
wt	36	67,33	110,83	15,83	0,17	1,67	6,83	4
tg	107	56,83	64,33	10,67	0	1,17	6,17	3,17

Table 5: Quantitative comparison of CR-positive interneurons in transgenic mice and wildtype mice

CR	Subiculum	St. oriens	St. pyramidale	St. radiatum	St. lac/mol	St. mol	St. granulosum	Hilus
wt	32,33	47,67	89	70,83	21,5	4,83	2,17	24
tg	68,67	37,17	53,17	41,83	20,17	20,33	46,67	28,5

Table 6: Quantitative comparison of CB-positive interneurons in transgenic mice and wildtype

CB	Subiculum	St. oriens	St. pyramidale	St. radiatum	St. lac/mol	St. mol.	St. granulosum	Hilus
wt	70,17	194	115,67	93,33	10,33	5,67	0	2,33
tg	127	106	239	85,67	11,67	7,17	0,5	1,83

mice

Table 7: Quantitative comparison of SST-positive interneurons in transgenic mice and wildtype mice

SST	Subiculum	St. oriens	St. pyramidale	St. radiatum	St. lac/mol	St. mol.	St. granulosum	Hilus
wt	40,33	125,33	77,67	56,17	0	0	1,67	22,17
tg	55,5	128,33	52,33	30,67	0,33	0,17	0,5	29

9.2 Total number of marked interneurons in the hippocampus

Table 8: Total number of marked PV-positive interneurons in the hippocampus

PV	Subiculum	St. oriens	St. pyramidale	St. radiatum	St. lac/mol	St. mol.	St. granulosum	Hilus
wt	36	67,33	110,83	15,83	0,17	1,67	6,83	4
tg	107	56,83	64,33	10,67	0	1,67	6,17	3,17
hAPP	206,33	250,83	70,17	144,17	73,17	81,17	0	72,5
Coloc.	75,33	35	43,83	6,5	0	0,83	3,17	2

Table 9: Total number of marked CR-positive interneurons in the hippocampus

CR	Subiculum	St. oriens	St. pyramidale	St. radiatum	St. lac/mol	St. mol.	St. granulosum	Hilus
wt	32,33	47,67	89	70,83	21,5	4,83	2,17	24
tg	68,67	37,17	53,17	41,83	20,17	20,33	46,67	28,5
hAPP	200	261,67	200	164,33	114,17	135,83	0	105,7
Coloc	14,33	11,83	15,5	8	6,17	5,33	14,5	19,33

Table 10: Total number of marked CB-positive interneurons in the hippocampus

CB	Subiculum	St. oriens	St. pyramidale	St. radiatum	St. lac/mol	St. mol.	St. granulosum	Hilus
wt	70,17	194	115,67	93,33	10,33	5,67	0	2,33
tg	127	106	239	85,67	11,67	7,17	0,5	1,83
hAPP	218,33	176	400	159,33	57	69	0	69,67
Coloc	54,83	58,83	210,5	35,5	6	5,17	0	0,67

Table 11: Total number of marked SST-positive interneurons in the hippocampus

SST	Subiculum	St. oriens	St. pyramidale	St. radiatum	St. lac/mol	St. mol.	St. granulosum	Hilus
wt	40,33	125,33	77,67	56,17	0	0	1,17	22,17
tg	55,5	128,33	52,33	30,67	0,33	0,17	0,5	29
hAPP	290,83	299,33	191,5	209,33	77,67	89	0	87,17
Coloc	26,83	65	13,67	19,33	0,33	0,17	0	16,67

9.3 Ratio of CaBP-, SST- and hAPP- positive interneurons to average hAPP-positive interneuron-number of all stains per hippocampus-layer

Table 12: Ratio of CaBP-, SST- and hAPP -positive interneurons to average hAPP-positive interneuron-number of all stains per hippocampus-layer

	Subiculum	St. oriens	St. pyramidale	St. radiatum	St. lac/mol	St. mol.	St. granulosum	Hilus
hAPP (total)	228,87	246,96	165,42	169,29	80,5	93,75	0	83,75
PV	75,33	35	43,83	6,5	0	0,83	3,17	2
CR	14,33	11,83	15,5	8	6,17	5,33	14,5	19,33
CB	54,83	58,83	210,5	35,5	6	5,17	0	0,67
SST	26,83	65	13,67	19,33	0,33	0,17	0	16,67

9.4 Ratio of CaBP- and SST-positive and CaBP-, SST- and hAPP-positive interneurons in the hippocampus

Table 13: Ratio of CaBP- and SST -positive and CaBP-, SST- and hAPP-positive interneurons in the hippocampus

	Subiculum	St. oriens	St. pyramidale	St. radiatum	St. lac/mol	St. mol.	St. granulosum	Hilus
PV	70,40%	61,59%	68,13%	60,92%	0,00%	49,70%	51,38%	63,06%
CR	11,28%	31,83%	29,15%	19,13%	30,59%	26,22%	31,07%	67,82%
CB	43,17%	55,50%	88,08%	41,44%	51,41%	72,11%	0,00%	36,61%
SST	48,34%	50,65%	26,12%	63,03%	100,00%	100,00%	0,00%	57,48%

10 Statutory Declaration

I declare on oath that I completed this work on my own and that information which has been directly or indirectly taken from other sources has been noted as such. Neither this, nor a similar work, has been published or presented to an examination committee.

Mittweida, 28.08.2017 Emira Shehabi

Location, Date Name Surname